# Engineering PLGA Nanoparticles for the Delivery of Genetic Tools: Toward mRNA-Based Gene Therapy

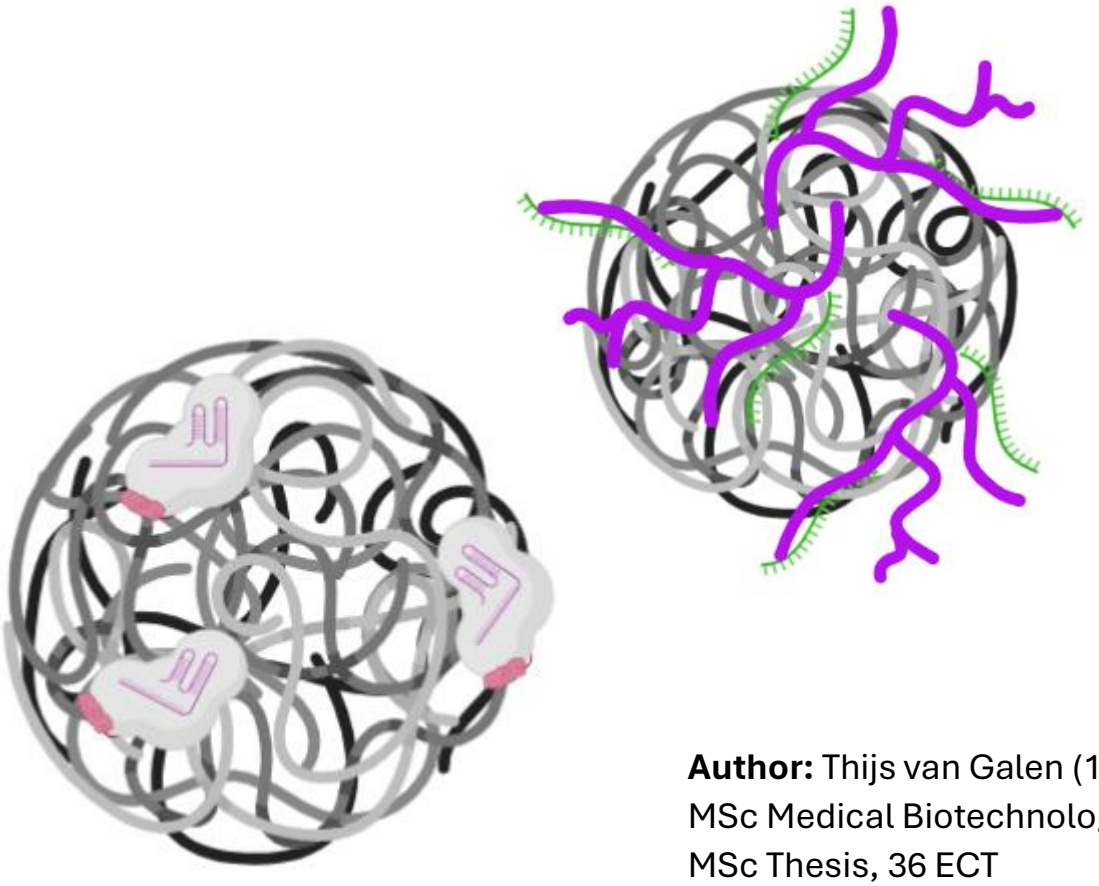

**Author:** Thijs van Galen (1034248)
MSc Medical Biotechnology
MSc Thesis, 36 ECT
**Supervisors:**

- Alvja Mali
- Mangala Srinivas

**Chair group:** CBI80436
**Date:** September 2024 – March 2025

# Table of Contents

## Abstract

Gene therapy has emerged over the past two decades as a promising approach for treating genetic diseases through single-gene modifications. To achieve precise genome editing, gene editing tools, such as CRISPR and base editors, are typically delivered in the form of mRNA or ribonucleoprotein (RNP) complexes, eliminating the risk of plasmid integration. Delivery of these platforms is often achieved through encapsulation in viral or non-viral vectors, which protect the cargo from premature degradation in the serum or body. Recent studies have increasingly focused on non-viral delivery systems, particularly lipid and polymeric nanoparticles (NPs), due to their reduced immunogenicity and improved loading capacity. This study investigates the feasibility of encapsulating RNP complexes in PLGA nanoparticles (NPs) and evaluates the impact of the double emulsion solvent evaporation method with sonication on both the stability of the RNP complexes and the integrity of the mRNA. While RNP complexes were successfully encapsulated, the RNP-loaded NPs did not induce the desired genetic modification in target cells. In contrast, GFP-mRNA-loaded NPs successfully transfected RAW 264.7 macrophages, leading to low levels of GFP expression. Our results demonstrate that the double emulsion solvent evaporation method, with sonication, can effectively encapsulate mRNA without significant degradation. This proof of concept highlights the potential of protein-encoding mRNA-loaded NPs as versatile delivery vectors for genetic modification and gene therapy.


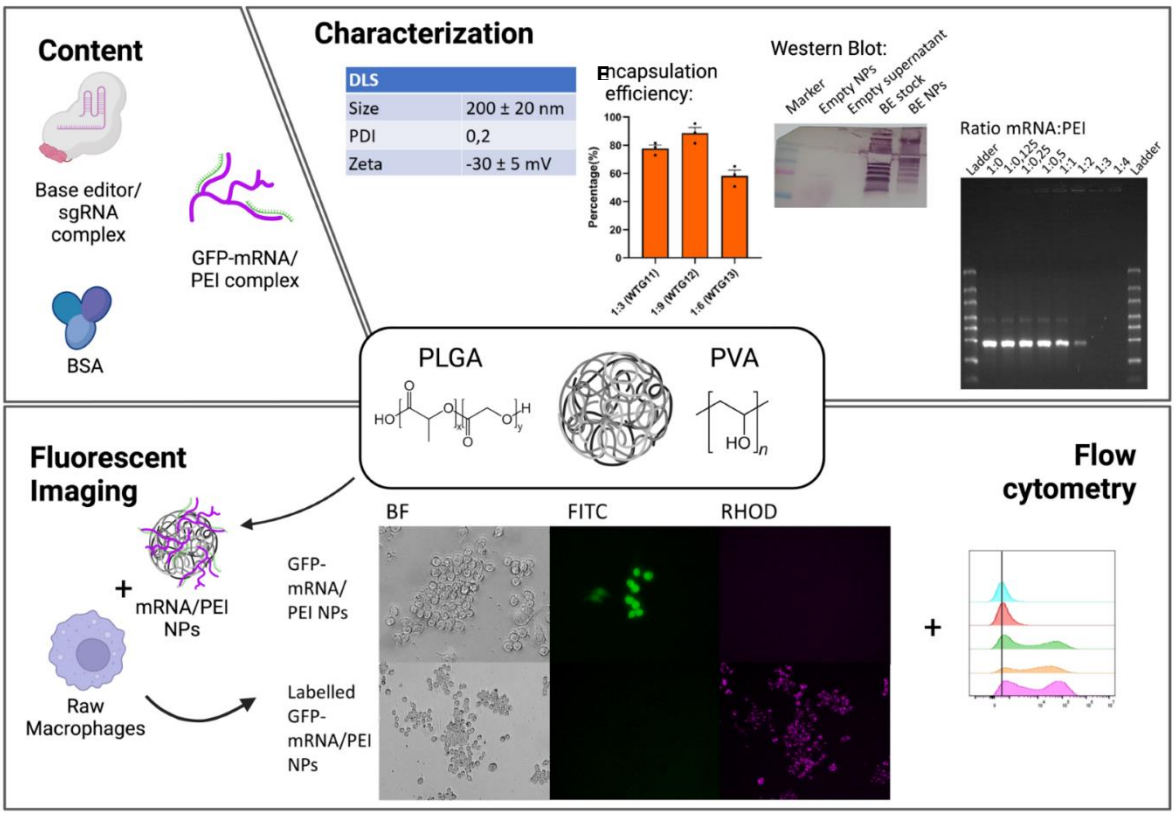


*Figure 1: The graphical abstract*

## List of Abbreviations

| | |
|---|---|
| BE | Base Editor |
| BCA | Bicinchoninic Acid assay |
| BSA | Bovine Serum Albumin |
| CRISPR | Clustered Regularly Interspaced Short Palindromic Repeats |
| Cy3 | Cyanine 3 |
| DCM | Dichloromethane |
| DEE | Direct Encapsulation Efficiency |
| DLS | Dynamic Light Scattering |
| (E-)NP | (Empty) Nanoparticles |
| E-sup | Empty supernatant |
| FGmRNA | French Guy GFP-mRNA |
| GFP | Green Fluorescent Protein |
| IEE | Indirect Encapsulation Efficiency |
| LNP | Lipid Nanoparticle |
| (L-)mRNA | (Labelled-) messenger RNA |
| PDI | Polydispersity Index |
| PEG | Polyethylene Glycol |
| PEI | Polyethylenimine |
| PLGA | Poly (lactic-co-glycolic acid) |
| PNP | Polymeric Nanoparticle |
| PVA | Polyvinyl Alcohol |
| RNP | Ribonucleoprotein |
| sgRNA | Single-guide RNA |
| TALEN | Transcription Activator-Like Effector Nucleases |
| W1/O/W2 | First water phase/Organic phase/Second water phase |
| ZFN | Zinc Finger Nuclease |

# 1. Introduction

There are over 4,000 mutations in protein coding genes that are known to be related to specific human genetic diseases [2]. Genome editing has revolutionized the field of genetics by offering precise tools to modify the DNA of living organisms. These gene editing tools have the potential to correct a wide range of genetic diseases, such as muscular dystrophy, sickle cell disease and certain types of cancer [3]. In particular, genetic diseases caused by single gene mutations, are predicted to be treatable with gene editing tools [4]. Since the discovery of the first gene editing tools two decades ago, there have been three generations of tools developed. The first and second generation, zinc finger nucleases (ZFNs) and transcription activator-like effector nucleases (TALEN) respectively, were promising genome editing tools, but they were difficult to design [5]. ZFNs were effective in some applications but not widely adopted due to the complexity involved in designing and validating the proteins for specific DNA targets. Similarly, while TALENs offered an easier alternative to ZFNs in terms of production and validation, challenges with protein design, synthesis, and validation still prevented them from being routinely used. However, the third generation, clustered regularly interspaced short palindromic repeats (CRISPR), have become a widely used approach for gene editing tools, offering potential cures for many genetic diseases [6].
Among the CRISPER systems, CRISPR/Cas9-mediated genome editing is one of the most extensively studied types, which typically consists of an endonuclease protein (such as Cas9 or Cas12) and a short guide RNA (sgRNA) which directs the nuclease to a specific DNA sequence via complementary base pairing [7]. There are different types of endonucleases which can induce insertions or deletions that are repaired via non-homologous end joining or homology-directed repair. However, there are several variations of the Cas9, for instance Cas9 nickase (nCas), which binds DNA with help of the sgRNA but does not induce double-strand breaks. When coupled to single-stranded DNA modifying enzyme, nCAS forms a base editor (BE) (Figure 1). Base editors enable precise point mutations by introducing single-base corrections [7]. Given these characteristics, base editors emerge as an exceptionally appropriate tool for correcting the single-nucleotide mutation necessary for instance in case of sickle cell disease. The characteristic sickle shape of the red blood cell, can be prevented by a single-nucleotide edit in the β-globin allele, which leads to a non-pathogenic phenotype [8].

Gene editing tools, such as CRISPR/Cas9 and BEs, can be delivered into cells through DNA plasmids, messenger RNA (mRNA), or directly as proteins [9]. These delivery methods differ primarily in expression duration, with DNA having the longest and protein the shortest. While DNA plasmids are more stable compared to mRNA-based delivery systems, they pose significant disadvantages for therapeutic applications, including the risk of unintended genomic integration and prolonged protein expression, which increases the chance of off-target effects [9]. mRNA delivery, in contrast, eliminates the risk of genomic integration and is gradually eliminated from the body over time, resulting in shorter expression and a reduced chance of off-target effects. Lastly, CRISPR/Cas9 can be delivered in the form of a ribonucleoprotein (RNP) complex, consisting of the Cas9 protein and the sgRNA. The RNP complex acts the fastest, as no transcription or translation is needed, further reducing off-target mutations compared to plasmids [10]. Moreover, the RNP complex is cleared the fastest, with the Cas9 protein being nearly undetectable 24 hours post-transfection, according to a study by Kim et al. (2014). However, excessively short expression durations may limit editing efficiency[9]. As a result, mRNA or RNP complexes have become more popular in genetic

modification therapies and research [9, 11]. However, a recent study focused on the comparison of targeted delivery of CRISPR/Cas9 RNP complexes and CRISPR/Cas9-encoding mRNA [12]. In this research, RNP-loaded nanoparticles (NPs) led to the unexpected death of all treated mice within two days, likely due to a strong immune response. While mRNA-loaded NPs effectively induced gene editing in 60 % of the liver cells, without observing negative health effects.

All three of the above-mentioned platforms commonly rely on vectors to improve cell entry, protect cargo from premature degradation, and improve the circulation time [11]. Delivery vectors can be divided into three categories: viral, non-viral, and mechanical (Figure 1). The latter can be used in combination with either of the others [13]. In 2022, viral vectors account for nearly 70% of all gene therapies in clinical trials and on the market [13]. These vectors are generally modified attenuated viruses in which viral genetic material is replaced with the gene of interest, in the form of DNA or RNA [11]. While viral vectors offer high transfection efficiency, they also have significant disadvantages, including strong immunogenicity, limited packaging capacity, and complex manufacturing processes, limiting their use is gene therapies. [11, 14].
These limitations have driven the development of numerous non-viral vectors, which offer lower immunogenicity, reduced toxicity and larger package capacity[13]. Among these, cationic lipid and cationic polymeric based particles are the most commonly used for gene therapy. Lipid nanoparticles (LNPs) can be formulated with a wide range of lipids in varying ratios to optimize factors like cellular uptake, encapsulation efficiency, and cell targeting [15]. Over time, LNPs have evolved into the most advanced methods for mRNA delivery, especially in vaccines and liver-targeted therapies [16, 17].

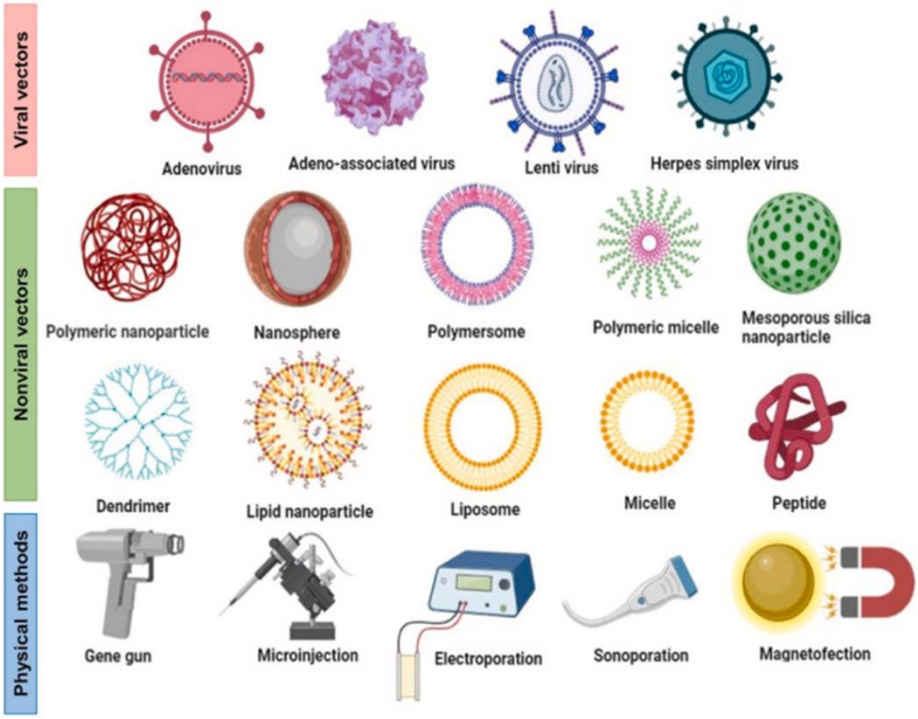


***Figure 2: The three types of vectors used for drug delivery: viral, non-viral and physical[1].***

Similar to LNPs, polymeric nanoparticles (PNPs) can consist of a variety of polymers or polymer mixtures, tailored to specific applications [1, 18]. Polymeric NPs are considered some of the most promising synthetic materials for nucleic acid delivery [1]. This is mainly due to their simple synthesis and functionalization, structural versatility, and scalability for large-scale production. Additionally, PNPs have low immunogenicity and good biocompatibility compared to viral vectors and inorganic NPs.

Non-viral vectors, including LNPs and PNPs, have one major disadvantage compared to viral vectors, which is lysosomal escape. Viruses, and therefore viral vectors, have developed complex biological mechanisms for cellular uptake and endosomal escape, resulting in their high transfection efficiency [19]. Additionally, the viral capsid protects the content from the acid pH present in the lysosome. However, non-viral vectors do not contain these mechanisms and are therefore dependent on other escape strategies and/or surface modifications to increase transfection efficiency. Although the mechanism is not yet fully understood, endosomal escape by LNPs is hypothesized to rely on ionizable lipids, which become protonated in the acidic endosomal environment [20]. These protonated lipids interact with anionic lipids of the lysosomal membrane, causing damage in the membrane and releasing the LNPs content into the cytosol. Another theory is known as the "proton sponge effect", which is dependent on the activation of proton pumps by the buffering capacity of LNPs [20]. Chloride ions are diffused into the lysosome, to achieve membrane equilibrium, increasing osmotic pressure leading to swelling and subsequent bursting of the lysosome. The proton sponge effect is also one of the four proposed endosomal escape mechanisms of PNPs, where pH buffering cationic materials, such as chitosan and polyethylenimine, induce proton pump activation, consequently leading to bursting of the lysosome [21, 22].

One of the most successful and well-described PNPs is the lactic-co-glycolic acid (PLGA) [18]. PLGA is biodegradable by hydrolysis into endogenous monomers, lactic acid and glycolic acid, making it a non-toxic compound and an FDA-approved material [23]. The degradation rate of PLGA can be adjusted from a week to several months by modulating the molecular weight and the ratio of the two monomers [23]. As a result, PLGA-based drug delivery systems can be engineered to release their therapeutic payload in a controlled and sustained manner. PLGA has been used to deliver a wide range of therapeutic molecules, including drugs, protein, peptides, mRNA, siRNA and plasmids [18, 24-27].

The most commonly used production method of PLGA NPs for protein and peptide encapsulation is the double emulsion solvent evaporation method [23]. This method was in a couple of studies successfully used to encapsulated CRISPR/Cas9 complexes in PLGA NPs [18, 28]. Cruz et al. 2021 describes a process in which guide-RNA was first precipitated in calcium phosphate before being co-encapsulated with the Cas9 protein in the PLGA NPs. After which, CRISPR/Cas9-loaded PLGA NPs successfully mediated gene editing in human erythroid cells. On the other hand, Srivastav et al. (2020) simplified the encapsulation process by pre-complexing the CRISPR/Cas9 protein with sgRNA before loading it into PLGA NPs.

The alternative to RNP-based delivery is the encapsulation of mRNA encoding for CRISPR/Cas9 in PLGA NPs. There are multiple studies that successfully encapsulate siRNA and mRNA in PLGA NPs with help of the polymer polyethylenimine (PEI) [22, 27, 29]. The positively charged PEI enhances RNA encapsulation and protection by electrostatically complexing with the negatively charged RNA, leading to its condensation and protecting it from degradation [22, 27]. Furthermore, PEI provides

pH-buffering properties, which facilitate the endosomal escape of the mRNA PLGA NPs via the proton sponge effect. However, PEI, especially high molecular weight and branched forms, can have high cytotoxicity [30, 31]. Another downside to mRNA encapsulation in PLGA NPs is the mechanical sheer stress derived from sonication and homogenisation during PLGA NP formulation, which may fragment mRNA, potentially reducing transfection efficiency [24, 32].

In the study by Cruz et al. (2021), PLGA NPs were effectively used as a vector for delivering CRISPR/Cas9 complexes for genetic modification in human erythroid cells. However, simplifying the encapsulation process and optimizing the PLGA NP formulation could enhance the scalability and feasibility of gene therapy on a larger scale. One key area that requires further investigation is the impact of the double emulsion solvent evaporation method using sonication on the stability of the RNP complex as this is unknown. Alternatively, mRNA encoding the base editor (BE) and sgRNA can be complexed with PEI and encapsulated in PLGA NPs. However, the effects of sonication on RNA integrity remain unclear. This raises the following research question: **How feasible is it to encapsulate the RNP complex in PLGA NPs, and what impact does the double emulsion solvent evaporation method with sonication have on the stability of the RNP complex and the integrity of mRNA?**
To answer this research question, the division into the following sub-questions can be made:

1. Is the RNP complex efficiently encapsulated, does it remain complexed, and does it retain functionality during nanoparticle formation using sonication?
2. How is the integrity of the RNA affected by the double emulsion solvent evaporation method using sonication?
3. How efficient is transfection of RNP complex PLGA NPs and mRNA NPs *in vitro*?

### *1.1 Hypothesis & Approach*

Based on previous research, successful encapsulation of RNP complexes in PLGA NPs is expected [18, 28]. However, the impact of sonication on the stability of the RNP complex remains unknown. The main concern for RNP complex encapsulation is the potential fragmentation of sgRNA due to mechanical sheer stress [24, 32]. Nevertheless, Sharifnia et al. 2019 was able to efficiently transfect human monocyte-derived dendritic cells with GFP-mRNA after 48 h, despite using sonication during NP formulation. Therefore, it is hypothesized that mRNA can be successfully encapsulated in PLGA NPs using sonication without affecting integrity, allowing for effective transfection.

To address these research questions, this study aims to simplify the encapsulation protocol previously described by Cruz et al. 2021 by pre-complexing the base editor and sgRNA into the ribonucleoprotein (RNP) before encapsulation in PLGA NPs via the double emulsion solvent evaporation method. The formulated RNP NPs will be characterised, encapsulation efficiency quantified, and transfection efficiency assessed using an *in vitro* model. Additionally, BSA- loaded NPs will be formulated, characterised, and BSA encapsulation quantified. The BSA-loaded NPs will serve as RNP model for optimizing protein encapsulation and protein quantification. Lastly, mRNA integrity will be tested by encapsulating GFP-mRNA in PLGA NPs, followed by characterisation, mRNA encapsulation quantification, and transfection efficiency on RAW macrophages using fluorescent microscopy and flow cytometry (Figure 1).

# 2. Materials and Methods

## 2.1 Materials

The following materials were used for particle formulation: PVA (9-10k MW, 80% hydrolysed, Sigma-Aldrich, bottle 7), PLGA (resomer 502H, Evonik), Dichloromethane (DCM, Sigma-Aldrich), MilliQ water, Nuclease free water (IDT, CAT#11050104), Adenine base editor (ABE8e NRCH protein, 180kDa) (ERASMUS Medical Centre), Makassar sgRNA (ERASMUS), BSA (Sigma-Aldrich, REF#10735086001), GFP-mRNA (OZBiosciences, REF#MRNA15), GFP-mRNA (gifted by French Guy), Polyethylenimine (PEI, branched 25kDa, Sigma-Aldrich CAT#408727), and Label IT® Nucleic Acid Labeling Kit (Mirusbio, CAT#MIR3600).

The following materials were used for SDS-PAGE and Western blotting: 6x SDS loading dye (378mM Tris-base (Invitrogen), 60% Glycerol (Merck), 12% SDS (Bio-Rad), 0.015% Bromophenol blue, and 600mM DTE), Any kD protein gel (Bio-Rad, CAT#4569033), Protein ladder (Bio-Rad, CAT#161-0374), GelCode Blue stain reagent (ThermoFisher, REF#24590), Semi dry transfer buffer (47.9 mM Tris-base (Invitrogen), 39.1 mM Glycine, 4.9 M Methanol, 1.3 mM SDS (Bio-Rad) in MilliQ water), Nitrocellulose blotting membrane (Amersham, CAT#10600002), Extra thick blot paper (Bio-Rad, CAT#1703969), TBS-T (Tris-Base, NaCl, Tween20 in MilliQ water), Blocking buffer (TBS-T with 5 % Non-Fat Dried Milk, Campina), Primary Ab (mouse anti-CRISPR/cas9, Novus biologicals, CAT#NBP2-36440), Secondary Ab (Goat anti-mouse AP, DAKO, REF#D0486), and AP substrate (Sigma-Aldrich, CAT#1002219239).

Protein assay Dye Reagent Concentrate (Bio-Rad, CAT#5000006) was used for protein quantification using the BCA assay.

The following materials were used for retardation assays, RNA gels, and RNA quantification: agarose (Eurogentec, REF#EP001005), TBE buffer (Tris-base, Boric acid, and EDTA), Quant-it RiboGreen Reagent (ThermoFisher, REF#R11491), RNA ladder and 2x loading dye (ThermoFisher, CAT#SM1821), and TE buffer (10mM Tris-HCl (ThermoFisher) and 1mM EDTA (Merck), adjusted to pH 7.5).

Lastly, the following materials were used for cell culturing, including flowcytometry: DMEM GlutaMAX medium (Gibco, REF#32480027, supplemented with 10% FBS, 1% Pen/Strep and 1% Sodium pyruvate), Trypan blue, PBS (Gibco, REF#10010015), FACS buffer (PBS (Gibco), 0.5 % BSA (Sigma-Aldrich), and 2 mM EDTA (Merck)), Compensation beads (Invitrogen, REF#01333342), CD16/CD32 rat anti-mouse FITC antibody (Clone 2.4G2, BD Pharmingen #CAT553144), Goat anti-mouse Cy3 antibody (Scientific laboratory supplies, CAT#PA43009), and Zombie Aqua viability kit (Biolegend, CAT#423101).

## 2.2 Methods

### 2.2.1 PLGA NPs Formulation

*Preparation and content of the first water phase*

PLGA nanoparticles (NPs) were prepared with the double emulsion solvent evaporation method, for which three phases were added together during sonication as described below in "Formulation of PLGA nanoparticles". The first water phase contained either BSA, BE/sgRNA (RNP) complex, GFP-mRNA, or water. Depending on the batch, ratios between phases and content was varied, which can be found in the appendix in Table S1. BSA batches were used for optimalization of the BCA assay protocol and finding the ratio between phases with the highest encapsulation efficiency. RNase free practices were followed wherever possible while working with RNA as mentioned by[28].

Before formulation of particles containing BE/sgRNA complexes, the complex was formed by incubating the BE and sgRNA in a molar ratio of 1:1.3 for 15 min at RT. The first and second water phase, as well as washing steps, were prepared using RNase free water.

In case of mRNA particles, four different types of content were entrapped in the batches: mRNA, labelled mRNA (L-mRNA), a mix between L-mRNA and mRNA, and previously mentioned types complexed with PEI. mRNA/PEI or L-mRNA/PEI complexes were formed by mixing the two together in ratios ranching from 1:0.266 to 1:0.798 (w/w mRNA/PEI), which was found with help of the retardation assay (see below), and incubating the mixture for 15-20 min at RT.

Labelling of mRNA with Cy3 was done with Label IT® Nucleic Acid Labelling Kit, following the protocol from the manufacturer (Mirus bio, Cat#MIR3600) and stored at -20 °C until further use. The labelling reaction was either incubated for 0,5h or 3h to create two different labelling densities.

NPs encapsulating only water, without RNP complex or mRNA, were prepared following the same protocol as described below. These empty nanoparticles (E-NPs) and the empty supernatant (E-supernatant) from the washing steps were used as control groups or to create blanks with similar contaminations as the other batches.

*Formulation of PLGA Nanoparticles*

NPs were prepared using the double emulsion solvent evaporation method as described in Cruz et al. 2021, with some modifications. In short, either RNP complexes, BSA, mRNA or water was encapsulated in the nanoparticles as mentioned above. In Figure 3 below, a schematic overview of NP preparation can be found.

The first water phase (W1), which contains protein, mRNA or water, was added to the organic phase (O), PLGA dissolved in DCM, to create the first emulsion (W1/O) using a probe sonicator (Branson S250 and Branson SFX550) on constant duty for 60 sec at 30 % amplitude while in an ice bath. A more detailed explanation of the first water phase can be found in the section 'preparation and content of the first water phase' above. Next, the first emulsion was added dropwise to the second water phase (W2) containing 1-2 % PVA while being sonicated for 60 sec at 30 % amplitude on ice, creating a double emulsion (W1/O/W2). Afterwards, DCM was evaporated by stirring the double emulsion for at least 3-4 h at 350 rpm at 4 °C. Then, the NPs were washed twice at 20100 rcf for 20-25 min at 4°C after resuspending in 1 mL water (5920R Centrifuge, Eppendorf). The supernatant from the washings was pooled and collected for indirect encapsulation efficiency analysis. The washed NPs were

resuspended in 1mL water and snap-frozen in liquid nitrogen, followed by lyophilization for at least 48h at -52°C. Lastly, the NP batches were weighed and stored at -20 °C.

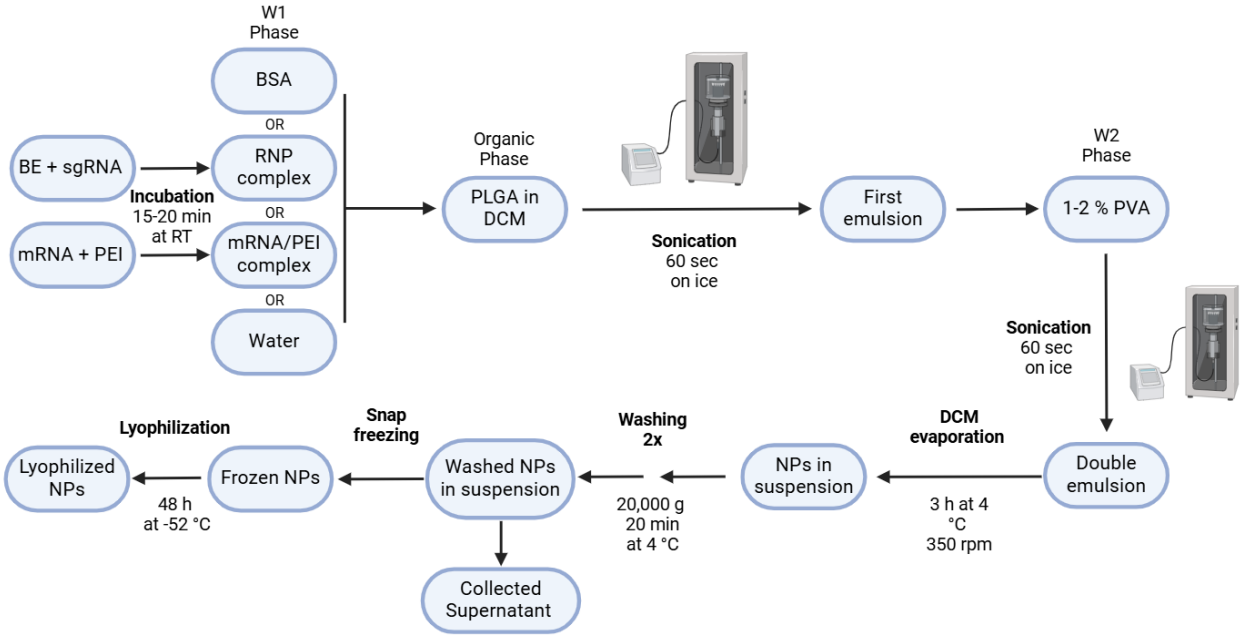


***Figure 3: A schematic overview of NP formulation.*** *Depending on the first water phase (W1), complexes were made by incubating for 15-20 min at RT. After which, the W1 phase was added to the organic phase and sonicated for 60 sec on ice, creating the first emulsion. The double emulsion was formed by dropwise addition of the first emulsion to 1-2% PVA solution during sonication for 60 sec on ice. The organic phase was evaporated for 3 h at 4 °C and residual components were washed away with 2 centrifugation washing steps at 20,000g for 20 min at 4 °C. The supernatant was collected and resuspended NPs were snap-frozen in liquid nitrogen, followed by lyophilization for 48 h at -52 °C.*

### 2.2.2 NP characterisation with dynamic light scattering

Characterization of the NPs, the size, PDI and zeta potential, was done by dynamic light scattering (DLS, Zetasizer 3, 270° angle). Samples were prepared in MilliQ to a final concentration of 0.1 mg/mL. The size of the samples was measured at 21 °C for four measurements of six 10-second runs after calibration of 120 sec. The zeta potential for samples was measured at 21 °C for four measurements of ten 10-second runs after calibration of 60 sec. The average was taken of the four measurements for size, PDI, and zeta for each sample.

### 2.2.3 SDS-PAGE and Western blotting for protein encapsulation confirmation

To confirm successful encapsulation of BE in NPs, SDS-page and Western blot were performed. To this end, 20 µL sample and 5 µL protein ladder were loaded on the SDS gel after 5 min of heating at 95 °C in sample buffer containing DTE. The gel was run until Bromophenol Blue reached the bottom of the gel, or until only the last four marker bands were left on the gel. The gel was washed three times for 10-15 min with MilliQ and either stained with GelCode Blue staining reagent for an hour, or the protein were transferred on a membrane using semi dry transfer blotting method (according to the protocol of CBI). Before the transfer, the gel, nitrocellulose membrane, and filter paper were soaked in transfer buffer for 10 min. A stack was made in the transfer cassette of the TransBlot SD system

(Bio-Rad) (from top to bottom): filter paper, gel, membrane, filter paper. Air bubbles in between the stack were removed and the blot was performed for 40min at 15V. The membrane was washed twice in TBS-T for 5min and blocked using blocking buffer (TBS-T containing 5% NFDM) for 1 h. The blocked membrane was incubated with the primary anti-Cas9 antibody in blocking buffer (1:1000 dilution) overnight at 4 °C. Next, the membrane was washed three times in TBS-T for 5 min and incubated with the secondary antibody (AP-goat anti mouse, 1:500 dilution) in blocking buffer for an hour. Lastly, AP substrate was poured over the membrane, and a photo was taken after 10 min when colouration on the membrane developed.

### 2.2.4 Protein quantification using BCA assay

The supernatant of BSA and BE batches was analysed to determine the encapsulation efficiency of protein indirectly. The BE supernatant was concentrated using a 100 kDa Amicon filter at 14,000 g for 10 minutes, as the protein concentrations were below the measurement threshold. A high or low range standard curve was made using a known concentration of BSA stock in Empty NP supernatant of the washings (E-supernatant). The high range (0.05 – 0.5mg/mL) assay was prepared by adding 10µL of standard curve or sample to a 96-well plate in triplicate. 200 µL of five times diluted Dye Reagent concentrate in MilliQ was mixed thoroughly with the samples and standard curve and incubated for at least 5min at RT. The low range (0.8 – 80 µg/mL) assay was performed by adding 160 µL of sample or standard curve in triplicate to a 96-well plate and mixing it thoroughly with 40 µL Dye Reagent concentrate and incubating it for at least 5 min at RT. After incubation the absorbance was measured at 595 nm with a Spectramax iD3 plate reader (Molecular Devices). The absorbance of the blank, E-supernatant, was subtracted from both the standard curve and the samples. The indirect encapsulation efficiency (IEE) was calculated from the obtained values, taking previous dilution and concentration steps in mind, with the following formula:

$$IEE = \frac{total\ amount\ of\ protein\ (mg) - free\ protein\ in\ supernatant\ (mg)}{total\ amount\ of\ protein\ (mg)} * 100$$

### 2.2.5 RNA gel electrophoresis and Retardation assay

In order to find the right ratio between PEI and mRNA where all mRNA is complexed, retardation assays were performed. For this 1g agarose was dissolved in 100 mL 1x TBE buffer using a microwave and let cool down to ±60 °C. 10 µL of RiboGreen Reagent was mixed through the solution before pouring the gel. The gel was loaded in the tray and submerged in 0,5x TBE buffer, after which 15µl sample or 3µL RNA ladder were loaded. Both samples and ladder were prepared in a 1:1 dilution with 2x RNA loading dye, while only the ladder was heated to 70°C for 5min. Before mixing the RNA samples with loading dye the mRNA was complexed with PEI in ratios ranging from 1:0.017 to 1:0.798 (w/w) and incubated at RT for 15-20 min. The gel was run at 100 V (5/6 V/cm between electrodes) for ±120 min or until Bromophenol Blue reached 2/3 down the gel. Photos were taken with Gel doc XR+ (Bio-Rad) using UV light and the SYBR safe filter. Afterwards the brightness and contrast of the photos were slightly adjusted with help of FIJI ImageJ (1.54g).

### 2.2.6 mRNA quantification with Quant-it RiboGreen Reagent

The indirect encapsulation efficiency (IEE) and direct encapsulation efficiency (DEE) of mRNA batches was determent with help of the RiboGreen RNA quantification assay described by the manufacturer (ThermoFisher, CAT#R11490) with some minor modifications. First, for the IEE, a high- or low-range assay and standard curve was made with mRNA in a mix of TE buffer and E-NP supernatant, representative to the concentration of contaminations in samples. Samples were either diluted in TE buffer in a dilution series or filtered with a 100 kDa Amicon filter at 14,000 g for 10 min and then diluted in a dilution series. High- (1 µg/mL to 20 ng/mL) and low- (50 ng/mL to 1 ng/mL) range standard curves were prepared with 2 µg/mL and 100 ng/mL mRNA stock solution respectively. Two reaction mixtures consisting of RiboGreen Reagent in TE buffer were made: a high-range, 200x dilution, and a low-range, 2000x dilution, reaction mixture. 100 µL standard curve or sample was added to a black 96-well plate in triplicate and 100 µL of corresponding reaction mixture was thoroughly mixed in the plate. The reaction was incubated for 5 min in the dark before measuring the fluorescence at excitation 480 nm and emission 520 nm with a Spectramax iD3 plate reader (Molecular Devices). The value of the blank, a mixture of E-NP supernatant and TE buffer, was subtracted from both the standard curve and the samples. An estimation of the IEE was made with the obtained values of the samples and the following formula:

$$IEE = \frac{total\ amount\ of\ mRNA - free\ mRNA\ in\ supernatant}{total\ amount\ of\ mRNA} * 100\%$$

Secondly, the DEE was determined by extracting mRNA from mRNA NPs described by Cun et al. (2011). In short, 2 mg of mRNA NPs, and E-NPs as control for the standard curve, were weighed and dissolved in 200 µL DCM, after which 500 µL TE buffer was added to the Eppendorf. The mRNA was extracted by end-over-end rotation for 90 min at RT and the samples were centrifuged at 20,000 g for 20 min at 4 °C. Next, the supernatant was collected, and residual DCM was evaporated at 37 °C for 5 min. A serial dilution was made for the samples, and the concentration was measured as described above for the IEE.

### 2.2.7 Cell culture

RAW macrophages (strain 264.7) were cultured to see the effectiveness of transfection of the mRNA NPs. The cells were cultured in T-75 flaks in DMEM GlutaMAX medium supplemented with 10 % FBS, 1 % Pen/Strep, and 1 % Sodium pyruvate at 37°C with 5% $CO_2$. At confluency, the cells were passaged to a new T-75 flask, every 3-4 days.

#### *Transfection of RAW macrophages*

For transfection experiments, RAW 264.7 macrophages were incubated for either 24 h or 48 h. The day before the treatment with NPs RAW cells were harvested, centrifuged at 500 rpm for 5 min and resuspended in new medium. The cells were counted with trypan blue (1:1 dilution) in a cell counter (Countess 3, Invitrogen). Next, the cells were seeded in duplicate in 24-well plates with a seeding density of 1,2*10^5 cells for 24 h treatment groups and with 0,8*10^5 cells for 48 h treatment groups, and incubated at 37 °C. On the day of the treatment, NPs were brought in suspension, by sonication in a water bath (Elmasonic P, Elma) for 5 min in non-supplemented DMEM medium and 5 mg

NPs/million of cells were added to the wells in duplicate and the plates were covered with aluminium foil and incubated at 37 °C. Two wells without NPs were taken along as control and for viability staining in flow cytometry experiments. 24 h post-treatment the 24 h and the 48 h conditions were washed 2-3 times with fresh medium to remove NPs. The 48-h condition plate was incubated for another 24 h at 37 °C. The effectivity of the transfection was either visualized with help of fluorescent microscopy or quantified with flow cytometry.

### *Visualisation of GFP expression and Cy3 presence using Fluorescent Microscopy*

After the transfection, fluorescence was visualised using fluorescent microscopy (Leica DMi8) with the lasers and filters for FITC (ex: 460-500 nm and em: 512-542 nm), Rhod (ex: 541-551 nm and em: 565-605 nm), and DAPI (ex: 327- 383 nm and em: 435-485 nm). The brightness and contrast of images was adjusted with the software FIJI ImageJ version 1.54g

### *Quantification of GFP expression using Flow Cytometry*

GFP expression and Cy3 presence was measured with flow cytometry (Cytoflex LX, Beckman Coulter). To this end, a protocol of CBI was followed. In short, the cells were washed twice in 400 µL PBS, after which the cells were scraped and transferred into two wells of a 96-well plate, two times 200 µL. All cells, except for 2 control wells, were stained with zombie aqua life/death staining in the dark for 30 min at RT. Meanwhile one drop of compensation beads was diluted in 300 µL FACS buffer, and 100 µL compensation beads were incubated with either 1 µL CD16/CD32 FITC antibody or Cy3 antibody for 30 min in the dark at RT. Next, 100 µL FACS buffer was added after staining and the cells and stained compensation beads were washed three times in 200 µL FACS buffer. The plate was loaded into the flow cytometer and events were measured at 30 µL/min for 5 min or until a total volume of 150 µL was reached. Fluorescence was measured with the filters B525 (FITC, 525/40), Y585 (PE 585/42), and V525 (KrO 525/40).
Data was gated as seen in Figure 4 below, in short, cells were selected by plotting the events in FCS-H/SSC-H, next single cells were selected by plotting SSC-A/SSC-H. With following gate, life cells were selected set with a positive Zombie Aqua control (DMSO) in FSC-A/com-KrO. Lastly, the gate for GFP positive cells was made by excluding all cells from the E-NPs control, plotting the compensated FITC against SSC-H. Gating and analysation was performed with FlowJo (version 10.10.0). The MFI in the compensated FITC channel was used to determine Percent Change, with the following formula:

$$Percent\ change\ (\%) = \frac{MFI\ of\ sample - MFI\ of\ control}{MFI\ of\ control} * 100$$

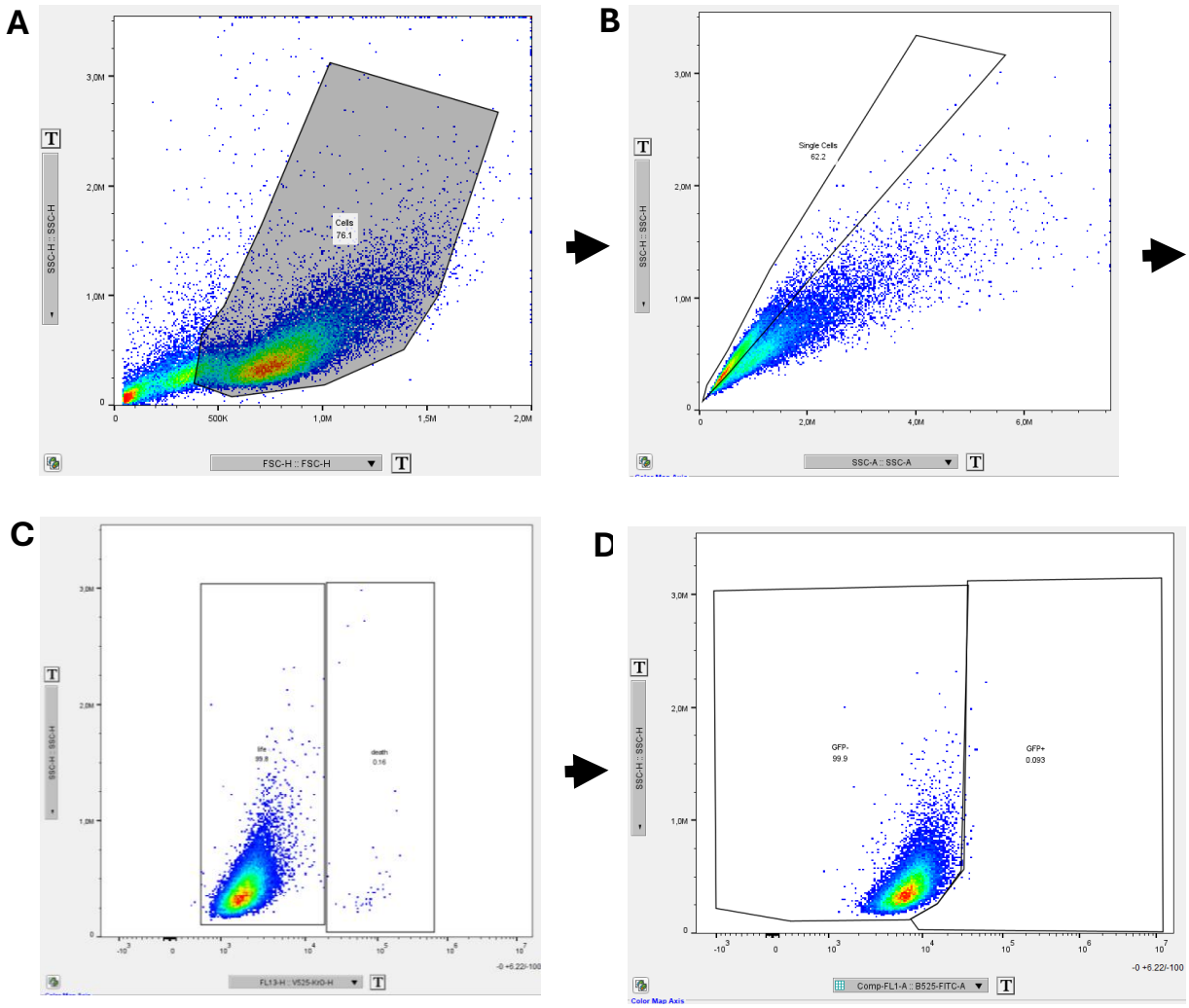


***Figure 4: Gating used during flow cytometry data analysis in FlowJo. A:*** *cells were selected by plotting the events in FCS-H/SSC-H* ***B:*** *single cells were selected by plotting SSC-A/SSC-H.* ***C:*** *Life cells were selected set with a positive Zombie Aqua control (DMSO) in FSC-A/com-KrO.* ***D:*** *The gate for GFP positive cells was made by excluding all cells from the E-NPs control, by plotting the compensated FITC against SSC-H.*

# 3. Results

In this study, PLGA nanoparticles (NPs) were formulated by encapsulating either RNP complex, BSA, or mRNA. RNP loaded NPs were the starting point of this study and were characterised and encapsulation efficiency was determined. RNP encapsulation was confirmed by SDS-PAGE and Western blot. Additionally, a collaborator tested transfection capabilities of RNP-loaded NPs on mutated erythroid progenitor cells. BSA loaded NPs were formulated as base editor (BE) model for optimizing protein encapsulation and protein quantification protocols. These BSA NPs were also characterised and analysed by SDS-PAGE. mRNA loaded NPs were used to determine the effect of PLGA NP formulation using sonication on the integrity of mRNA by determining the transfection efficiency on RAW 264.7 macrophages.
In this results section the findings are organized based on the type of NPs formulated, with each category further divided into two parts: characterization and quantification of the encapsulated content. Additionally, the transfection efficiency of mRNA-loaded NPs, as assessed by fluorescent microscopy and flow cytometry, is presented in the final section, following the encapsulation quantification results.

All DLS data was analysed using a consistent approach. The size and size distribution, known as polydispersity Index (PDI), were determined by averaging four measurements of each batch, after first examining the size distribution across intensity, volume and number graphs. If the size measurement followed a normal distribution without a second peak, the average of the size by intensity was used. However, in cases where abnormally large particles or residues present in the sample, the size and PDI based on number distribution were reported instead (see the example in Figure 5A/B/C). The zeta potential was also averaged after verifying the zeta potential distribution across four measurements (Figure 5D). A complete overview of the DLS data, along with additional details on phase ratios and encapsulated content for all batches, is provided in the appendix (Table S1).

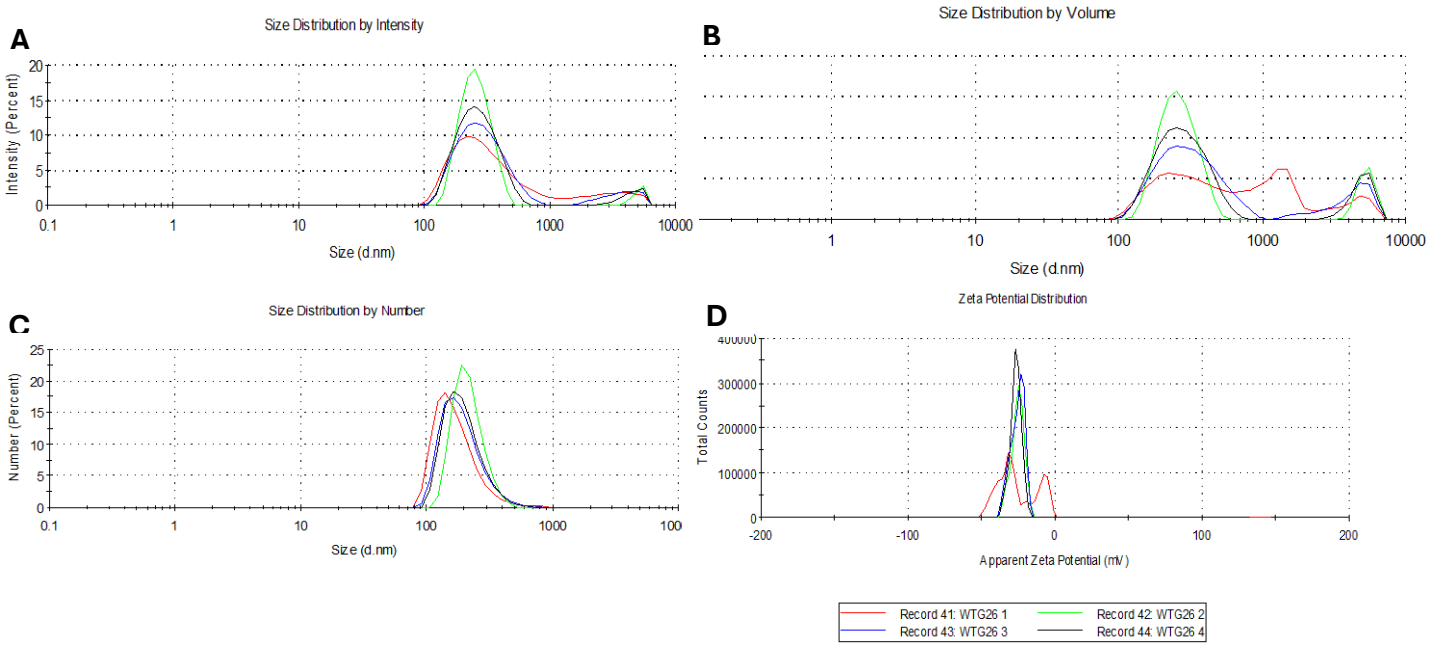

***Figure 5: An example of size and zeta potential distribution graphs (of batch WTG26).*** *Each sample is sample was measured four times and the distributions were plotted in the graphs.* ***A:*** *The size distribution by intensity, two peaks can be seen at roughly 250 nm and 5500 nm* ***B:*** *Size distribution by volume, the same two peaks are visible at ±250 nm and ±5500 nm* ***C:*** *Size distribution by number, the peak at ±250 nm has shifted forward to ±190 nm and the peak at ±5500 nm has disappeared* ***D:*** *The zeta potential distribution with an average value of the peaks at roughly -25 mV.*

## 3.1 RNP complex NPs

As starting point of this research, RNP complexes were formed and encapsulated in PLGA NPs as described in the materials and methods. The encapsulation efficiency of protein in the NPs was determined by quantifying the concentration in the supernatant of the washings, while successful encapsulation of protein in the NPs was confirmed using SDS-PAGE and Western blot analysis. Additionally, RNP complex NPs were sent to collaborators, which provided the RNP complex, for transfection efficacy testing.

### 3.1.1 Confirmation of successful RNP encapsulation with Western blotting and BCA assay

Western blot analysis was first performed on a dilution series of BE (base editor) stock in order to test the protocol and determine how the BE and positive control would look like at different SDS loading amounts (Figure 6A). The results demonstrated that the primary antibody successfully binds BE (180 kDa), however, multiple bands ranging from >250 kDa to <50 kDa were observed. These bands gradually decrease in intensity at higher dilutions, with only one clear band at 180 kDa remaining at the highest dilution tested. Interestingly, the 180 kDa band was not visible in the left five lanes containing BE-loaded samples. Instead, a thick white band appeared, suggesting possible antibody binding interference or inhibition of AP substrate conversion. As the samples were further diluted, this white band gradually decreases in size, allowing a clear coloured band to appear at 180kDa for the 0.06 µg-loaded sample. This finding confirms that the primary and secondary antibodies used were functional.

Secondly, to validate RNP encapsulation in the NPs batch named WTG05, Western blot analysis was performed on both the NPs and the supernatant, which can be seen in Figure 6B. In the second and third lane of the Western blot empty NPs (E-NPs, meaning PLGA NPs without the BE) and Empty supernatant (E-supernatant, meaning the supernatant obtained from the washings of E-NPs) served as negative control, and no AP substrate conversion was observed in these lanes, indicating no non-specific antibody binding to the compounds used for NP formulation itself. The BE stock (180kDa), used as a positive control, which can be seen in the fourth lane, and showed strong colouration of the AP substrate, consistent with the bands observed in the BE dilution series (Figure 6A). All lanes containing RNP NPs or RNP supernatant from washings showed conversion of AP substrate confirming successful encapsulation of BE in the NPs. An attempt to partially dissolve the NPs with DMSO so the RNP would be released from the NPs, resulted in distorted and vaguer bands in the Western blot. Additionally, RNP supernatant did not seem to run correctly on the SDS-PAGE gel, as no band was visible at 180 kDa (Figure S1 in the appendix).

By comparing the band width of the white band at 180 kDa of RNP NPs to the dilution series in Figure 6A, the amount of RNP released from the NPs can be roughly estimated. The band size of the white band in '200 µg RNP NPs' in Figure 6B was similar to the 0.25 - 0.5 µg BE loaded lanes in Figure 6A, corresponding to an estimated 1-2.5 ng of RNP per µg of NPs in batch WTG05.

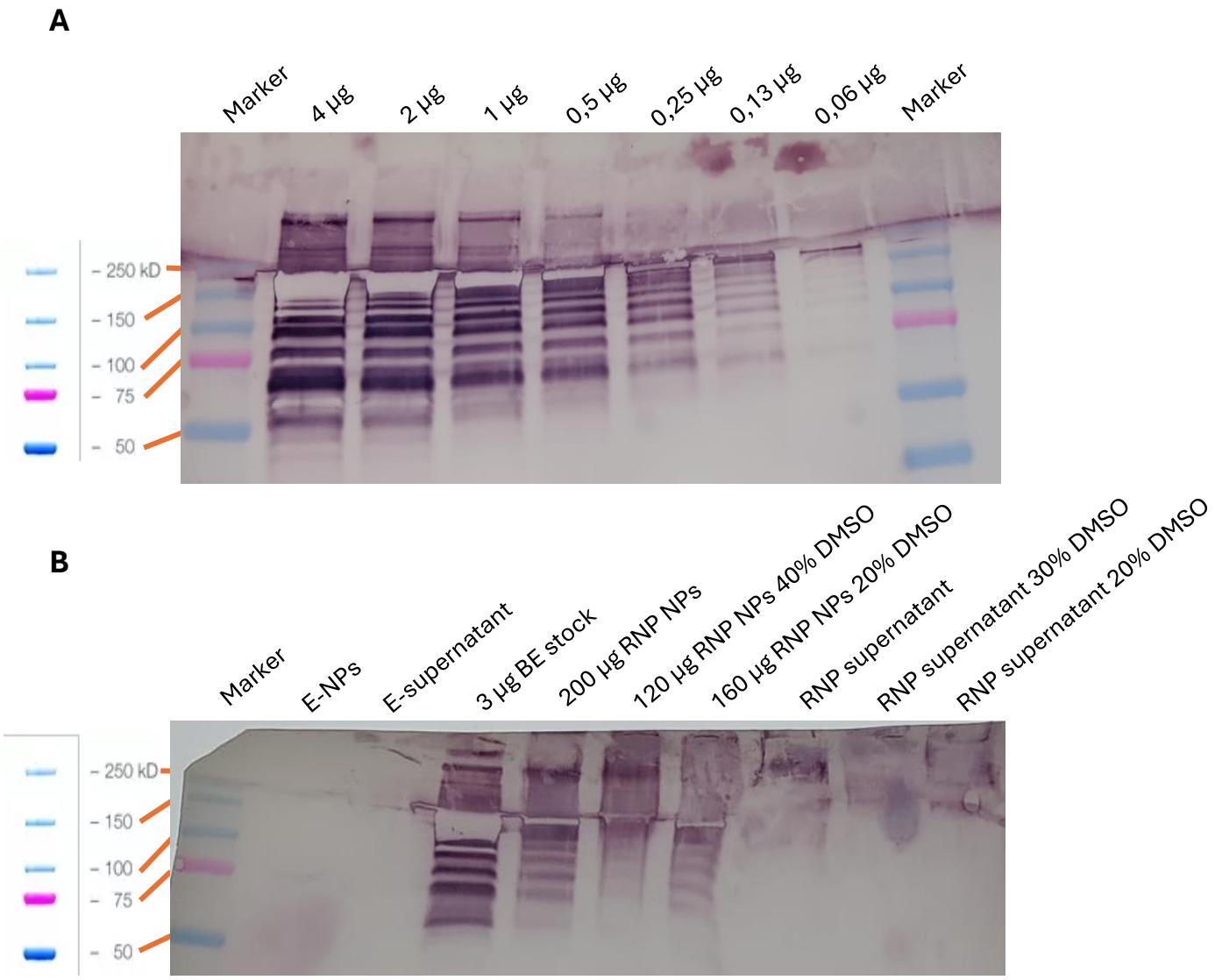


***Figure 6: Western blot of dilutions series of BE stock (180kDa) (A) and a Western blot of RNP complex loaded NPs (batch WTG05) with empty NPs as control (B). A:*** *the lanes form left to right decrease in total amount of BE loaded on the SDS-PAGE gel, which can be found on top of each lane. A strong colouration of AP substrate can be seen with multiple bands present in each lane ranging from <50kDa up to >250kDa, with a white band at the height of the size of the BE, 180kDa. As the bands colouration decreases at higher dilutions, the white band becomes smaller in size and turns purple at the highest dilution (0.06 µg), while other bands present fade away.*
***B:*** *The lane from left to right: Protein marker, Empty NPs, supernatant of empty NPs, BE stock solution, 200 µg of RNP NPs, 120 µg of RNP NPs resuspended in 40% DMSO, 160 µg RNP NPs resuspended in 20% DMSO, supernatant of RNP NPs, RNP supernatant in 30% DMSO, and RNP supernatant in 20% DMSO. The BE has a size of 180kDa. No BE is present in the positive controls (E-NP and E-supernatant) and for other samples colouration of the AP substrate indicate that there was BE specific antibody binding.*

### 3.1.2 Contaminants cause problems for protein quantification in supernatant

Next, the goal was to quantify the amount of RNP-loaded in the NPs during formulation, referred to as the indirect encapsulation efficiency (IEE). To this end, Nanodrop and Qubit protein measurements were used to determine the non-encapsulated RNP in the supernatant.
However, the protein concentrations measured in the supernatant using both methods, Nanodrop N60 (Implen) and Qubit 4 (Invitrogen), was higher than theoretically possible (Figure 7). Due to the low amounts of RNP added in the W1 phase (first water phase) of the NP preparation, the protein concentration in the supernatant of the washings was typically too low to measure directly. To address this, the supernatant was fist concentrated, and as a control, the concentrate was then diluted again to check whether the measured concentration dropped accordingly. Unexpectedly, for all the samples tested, the measured values remained higher than the maximum theoretical value that could have been present in the supernatant if no RNP was entrapped. Additionally, all RNP supernatant samples analysed using Nanodrop triggered a contamination warning, with A260/280 ratios exceeding 1.5, significantly higher than the expected protein ratio of >0.57, according to Nanodrop specifications. Thus, these findings indicated that measurements obtained with Nanodrop or Qubit did not represent the actual protein concentration in the supernatant.
The Qubit was also used to measure the RNA concentrations in control samples in order to observe the effect of PLGA NPs and BE on the measurement (appendix Table S2). This data suggested that PLGA NPs present in the sample did affect RNA concentrations measured, however the addition of BE did reduce the measured RNA concentration with ±40 ng/µL. Additionally, 0.05 mg/mL E-NPs without RNA, gave high background signal.

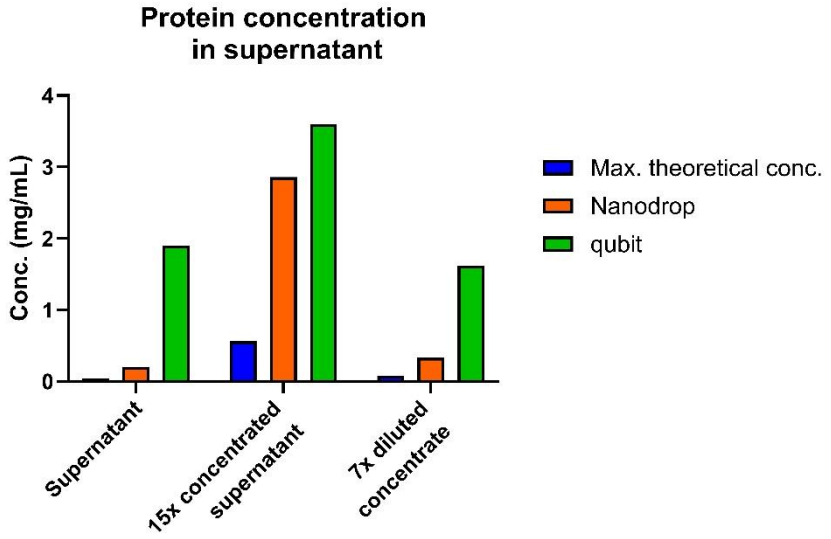


***Figure 7: The protein concentration in the supernatant of WTG05*** *compared to the highest possible theoretical concentration it could have if no protein was encapsulated in the NPs (in blue). In orange Nanodrop measured values and in green Qubit measured values are shown for three different samples. Supernatant of WTG05 without further processing, Supernatant after concentrating 15 times with 100kDa Amicon filter, and a 7 times dilution of this concentrated supernatant.*

Since Qubit and Nanodrop measurements were unreliable compared to the maximum theoretical values, a BCA assay was performed as an alternative. The concentration of RNP in the supernatant of the washings was calculated to be 32,04 µg. From this concentration the IEE can be determined, which was 58% (Table 1). The standard curve used for IEE of batch WTG05 is provided in appendix Figure S2A.

***Table 1: BCA assay of RNP batch WTG05***.

| Sample name | Measured RNP conc. in concentrated Supernatant (µg /µL) | RNP conc. in supernatant (µg /µL) | Total amount of protein in supernatant (µg) | IEE (%) |
|---|---|---|---|---|
| WTG05 (74 µg BE) | 0,24 | 0,008 | 32,04 | 58 |

### 3.1.2 Unsuccessful in vitro trial of RNP NPs

A portion of the RNP batches (WTG02 and WTG05), was sent to collaborators, which provided the encapsulated BE, for testing on an erythroid progenitor cell line carrying the mutation of interest. The cells were treated with RNP-loaded NPs using two methods. In the first method, cells were exposed to three different NP concentrations for 48 hours. After treatment, the cells were washed, the culture medium replaced, and the cells were cultured for an additional 5 days to allow for expansion before harvesting for genome editing analysis. In parallel, cells were nucleofected with two different NP concentrations to assess genome editing independent of NP uptake. After 24 hours, cells were washed, the medium replaced, and they were cultured for 6 more days before harvesting for analysis. Despite these treatments, no detectable genome editing was observed in either the treated or nucleofected cell populations upon subsequent analysis. Given the lack of efficacy, along with the degradation and aggregation observed in the Western blot analysis, the decision was made to switch to mRNA-loaded NPs.

## 3.2 BSA NPs

BSA- loaded NPs were formulated alongside the RNP NPs for two main reasons:

1. To identify the optimal ratio between the W1 (aqueous), O (organic) phases that resulted in the highest indirect encapsulation efficiency (IEE).
2. To serve as a control for BCA assay and SDS-PAGE analysis.

To this end, three different batches were prepared with varying ratios of the W1 phase to the O phase: 1:3, 1:9, and 1:6, corresponding to WTG11, WTG12, and WTG13, respectively.

### 3.2.1 Finding the optimal ratio for protein encapsulation with Characterization & Quantification of BSA batches

The BSA concentration in the supernatant was determined using BCA assay, and the IEE was calculated (Figure 8). Batch WTG12 (W1/O ratio of 1:9), exhibited the highest IEE of 89%, whereas WTG13 (W1/O ratio 1:6) had the lowest IEE of 59%. These findings suggests that a W1/O ratio of 1:9 is optimal for protein encapsulation. Therefore, this ratio was chosen for the subsequent mRNA NP formulation.

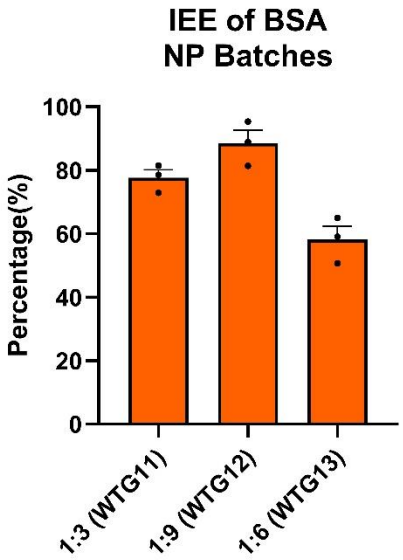


***Figure 8: The IEE of BSA NP batches with different W1/O ratios*** *based on BSA concentrations in the supernatant of the washings determined with BCA assay. The ratio of 1:3 (WTG11) between W1 and O resulted in an IEE of 77 %, for 1:9 (WTG12) this was 89 %, and for 1:6 ratio (WTG13) the EE was 59 %.*

## 3.3 GFP-mRNA NPs

As the RNP NPs did not effectively induce genome editing, as mentioned above, a switch to messenger RNA (mRNA) was made. For this reason, green fluorescent protein mRNA (GFP-mRNA) NPs were formulated, and their transfection capacity was tested on RAW 264.7 macrophages using fluorescence microscopy and flow cytometry.

### 3.3.1 mRNA/PEI ratios found with gel retardation assay

To improve transfection efficiency, mRNA was complexed with PEI before encapsulation in NPs, as PEI helps with lysosomal escape and protects mRNA from degradation. As PEI is cytotoxic in higher concentrations, it was necessary to determine the minimum weight ratio (w/w) required to fully complex all mRNA with PEI using a gel retardation assay. In this study, two GFP-mRNA were used: (i) a commercially available version and (ii) a gifted version from a collaborator referred in this report as French Guy (FG). Complex formation between mRNA and PEI is based on electrostatic interaction, where the positive charge of PEI binds to the negative charge of RNA. Therefore, the optimal mRNA/PEI ratio was determined separately for both commercial and FG GFP-mRNA and is shown in Figure 9A and 8B respectively. The results show that complete complexation of both GFP-mRNA types occurred at a 1:0.399 (mRNA: PEI) weight ratio, as indicated by the absence of an mRNA band at the same height as the positive control (uncomplexed mRNA) (Figure 9). The Figure shows also a size difference between the two mRNA strands: ±900 bp for commercial mRNA and ±1400 bp for FG-mRNA. Lastly, a gradually decreasing smear extending from the 1400 bp band in the positive control of FGmRNA, shown in Figure 9B, indicates partial degradation of the mRNA.

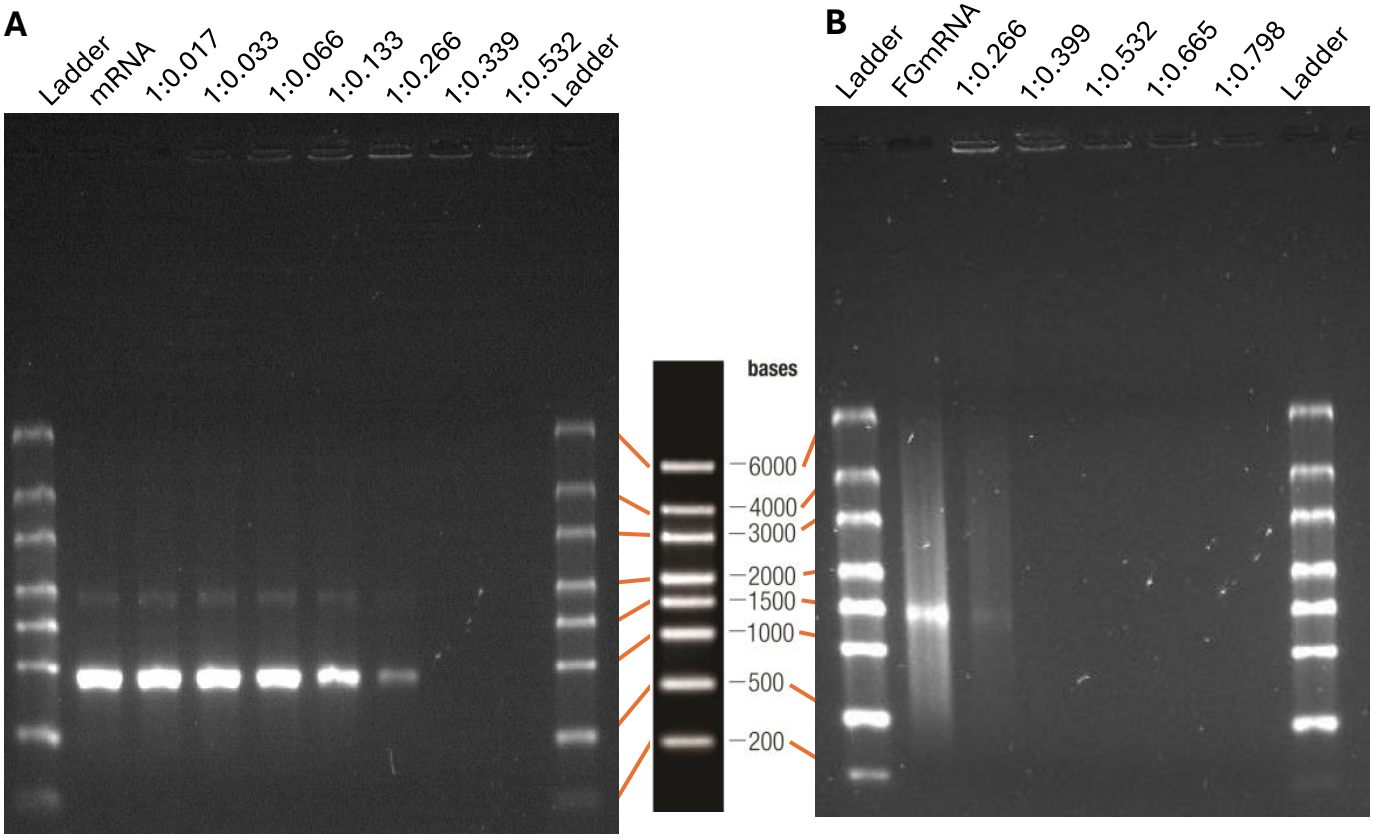


***Figure 9: Retardation assay of mRNA/PEI complexes of commercial GFP-mRNA (A) and gifted GFP-mRNA (B).*** *For both gel A and B in the second lane uncomplexed mRNA can be seen, on the right of this lane mRNA/PEI complexes were loaded with increasing (w/w) ratios. The w/w ratio of 1:0.339 in both gels prevent mRNA from running completely.*

During formulation of some of the mRNA loaded NPs batches, labelled mRNA (L-mRNA) was used, see appendix Table S1. Since both the linker of the Label-IT reagent and the Cy3 dye contain multiple nitrogen atoms with positive charges, an additional retardation assay was performed to determine the optimal mRNA/PEI ratio for L-mRNA. mRNA with two labelling densities, based on incubation time with Label-IT reagent, were made for encapsulation in PLGA NPs, as explained in the materials and methods. Therefore, the optimal L-mRNA/PEI ratio was determined for 0.5 h (Figure 10A) and 3 h (Figure 10B) incubation.

As shown in Figure 10, the L-mRNA/PEI ratio of 1:0.266 (w/w) was sufficient to fully complex L-mRNA under both labelling conditions. This ratio between L-mRNA and PEI (1:0.266) is lower than for unlabelled mRNA (1:0.339) as can be seen above in Figure 9, likely due to the extra positive charges introduced during labelling. Additionally, in Figure 10B, a small increase in nucleotide size was observed from ±1400bp to ±1500bp for L-FGmRNA compared to unlabelled FGmRNA, likely caused by the Cy3 conjugations of the high labelling density.

In conclusion, the minimum weight ratio for complete complexation of unlabelled mRNA with PEI was 1:0.339, while for L-mRNA the optimal ratio shifted to 1:0.266. These optimal ratios were used for all the subsequent formulations of mRNA NP batches.

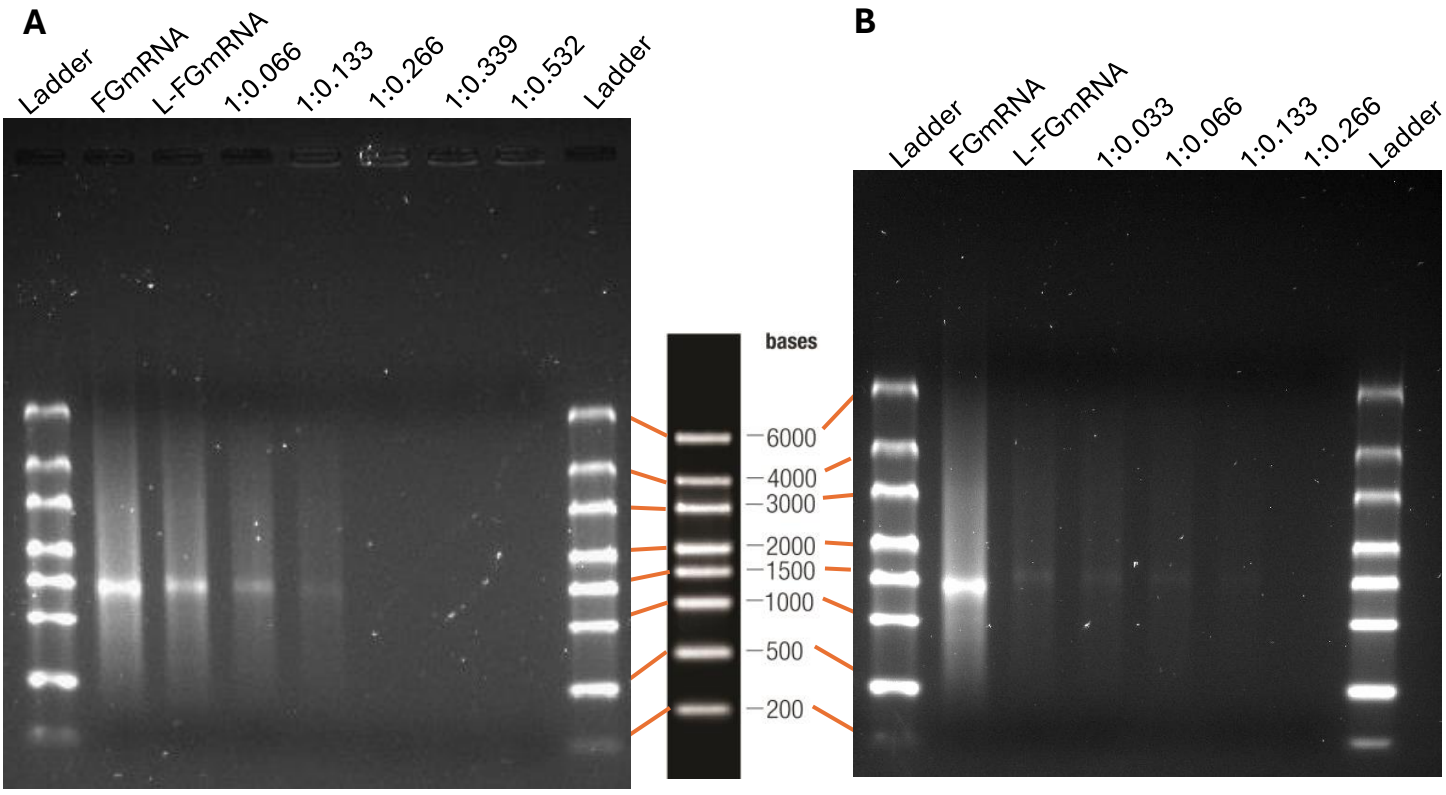


***Figure 10: Retardation assay of L-mRNA/PEI ratios. A: L-mRNA with an estimated labelling density of 1 label per every 40-120 bases of nucleic acid (0.5h incubation).*** *From left to right: ladder, unlabelled mRNA, L-mRNA, increasing L-mRNA/PEI ratios (w/w), and ladder.* ***B: L-mRNA with an estimated labelling density of 1 label per every 6.6-20 bases of nucleic acid (3h incubation and 6 times higher density than A).*** *From left to right: ladder, unlabelled mRNA, L-mRNA, L-mRNA, increasing L-mRNA/PEI ratios (w/w), and ladder. In both assays the w/w ratio of 1:0.266 prevents mRNA from running completely.*

### 3.3.2 Challenges of mRNA Quantification with RiboGreen quantification assay

Similar to protein encapsulation efficiency, the indirect mRNA encapsulation efficiency can be determined by measuring the concentration of mRNA in the supernatant of the washings. To this end, the RiboGreen RNA quantification assay was used, and standard curves were made with comparable concentrations of contaminating NP components, for which diluted Empty NP supernatant (E-sup) was used (Figure 11A). The contaminants present in the supernatant, PVA and PLGA, were found to increases RiboGreen fluorescent signal, as shown by the increased slope of the corresponding standard curves (Figure 11A). The slope of the standard curve in TE buffer without contaminants (the orange line) was over three times lower than the standard curves made using supernatant from Empty NP (E-sup), represented by the blue and green line. Furthermore, the assay demonstrated that complexing mRNA with PEI did not affect the fluorescence measured compared to the uncomplexed mRNA in the 1:20 E-sup and TE buffer mixture.

The impact of using an appropriate standard curve is also reflected in the calculated mRNA concentrations for the diluted WTG24 samples (Figure 11B). As shown, concentrations corresponding to the standard curve in TE buffer (in green) were over three times higher than those calculated using standard curves with contaminants. Additionally, mRNA concentrations did not decrease proportionally with 2x and 4x dilutions of the supernatant, as would be expected. These findings suggest that while contaminants strongly influence fluorescence and must be considered when preparing standard curves, PEI complexation with mRNA does not interfere with the RiboGreen assay. However, the mRNA concentrations calculated from supernatant of WTG24 suggested that they did not reflect reliable mRNA concentrations.

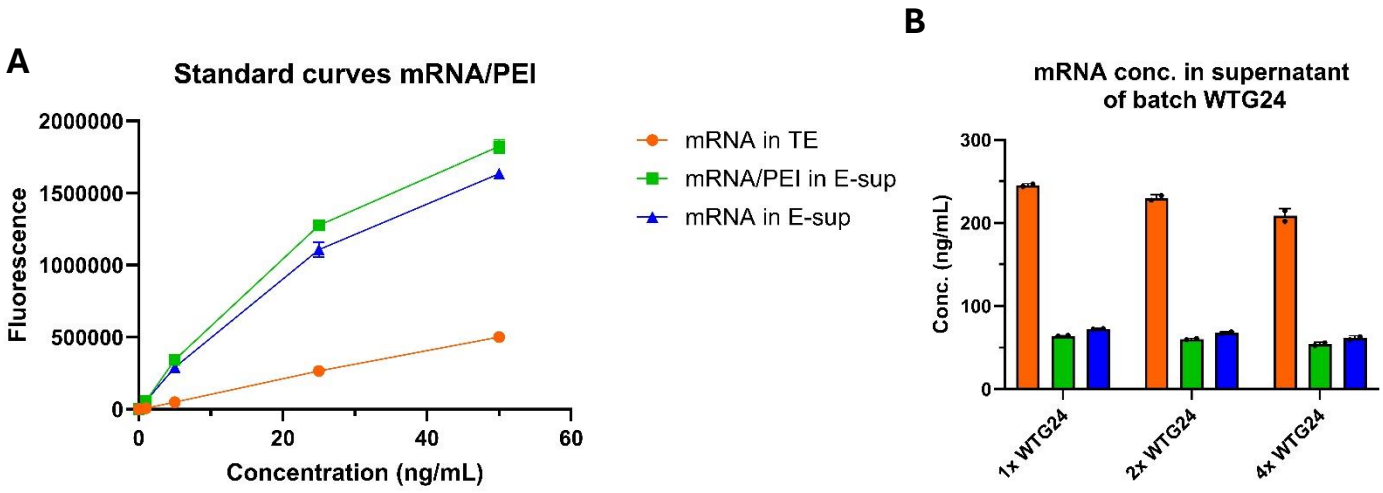


***Figure 11: Low range Ribogreen RNA quantification standard curves show the effect of contaminants (A) and corresponding measured mRNA concentration in supernatant of batch WTG24 (B).*** *As shown in the standard curves in A, contamination in the supernatant of the washings causes an increase in fluorescence measured, however mRNA/PEI complexation has little further effect. In B the effect of the use of different standard curves can be seen on the calculated mRNA concentration. Additionally, the drop in mRNA concentration is not equal to the dilutions made, suggesting unreliable results.*

To improve reliability, the supernatant of the washings was filtered in an attempt to remove some of the contaminants present. A test using a known concentration of FGmRNA in TE buffer (50 ng/mL) was performed to assess how much mRNA would be lost in the concentrated fraction with the contaminants and needed to be corrected for. In Figure 12 the calculated mRNA concentrations are shown, which were determined with the standard curve made with filtrated E-sup (see appendix S5A). The mRNA concentrations of unfiltered samples were 47.3 ng/mL and 25.7 ng/mL respectively, as expected. In contrast, the mRNA concentrations in the filtrated samples did not exceed 0,7 ng/mL, showing that the FGmRNA with a size of ±1400 bp (see Figure 9B) did not pass through a 100kDa Amicon filter. Therefore, filtering the supernatant of the washings prior to RNA quantification is not effective.

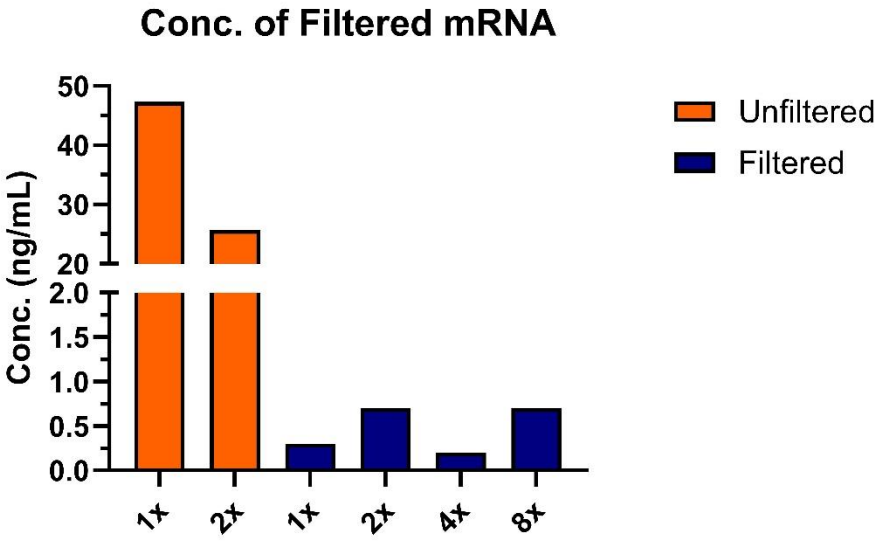


***Figure 12: Calculated mRNA concentration of unfiltered and filtered sample in a dilution series determined by Ribogreen RNA quantification assay****. A known amount mRNA was added to TE buffer to a final concentration of 50 ng/mL. Before filtering a sample was taken for the unfiltered samples (in orange) and the remaining sample was filtered (in blue) with 100kDa Amicon filter. Both filtered and unfiltered samples were further diluted, and concentrations were calculated with a standard curve made with filtrate of E-sup (appendix S5A).*

Lastly, an attempt was made to determine direct encapsulation efficiency (DEE) by extracting mRNA from mRNA NP batches. In this method contaminants, PLGA and possibly PVA, would remain in the organic phase, DCM, during the extraction while mRNA would end up in water phase (TE buffer). A representative standard curve was made using E-NP extract with a known amount of mRNA (appendix S5B). The results of the dilution series made with WTG36 extract are shown in Figure 13. Surprisingly, the highest concentrations in the series (1x, 2x, and 4x) yielded values of 0.26 ng/mL or lower. This was followed by an increase in concentration for the 8x and 16x diluted samples, which had values of 4.62 ng/mL and 6.77 ng/mL, respectively. However, the concentrations then dropped again to 2.28 ng/mL for the 32x diluted sample, and fell below zero for the remaining dilutions tested. Interestingly, the decrease from 6.77 ng/mL to 2.28 ng/mL between the 16x and 32x dilutions was the only instance in the series where two concentrations halved, as expected in the dilution series. The negative values for 64x, 128x, and 256x samples might suggest that these dilutions were below the detection range of the assay, 1 ng/mL.

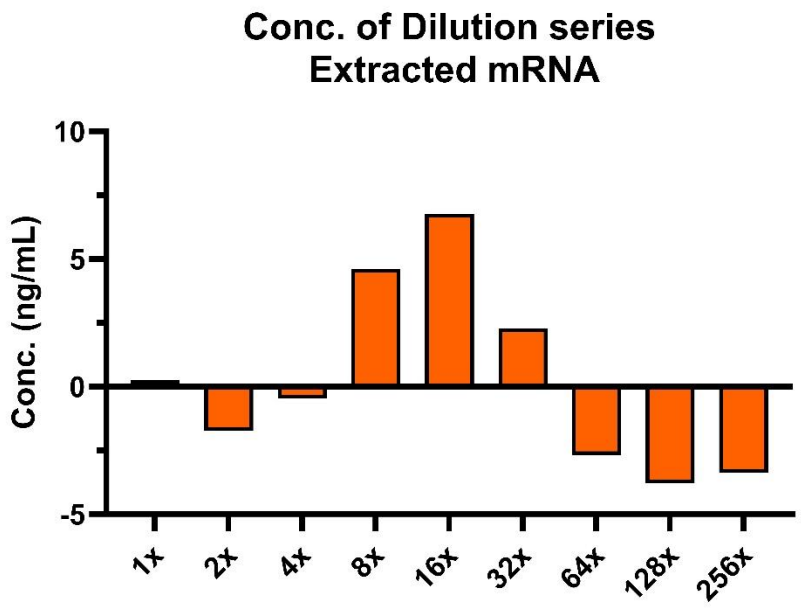


***Figure 13: RNA concentration of dilution series of extracted mRNA from 2.1 mg mRNA NPs*** *(batch WTG36). Negative concentrations can be seen for 2x, 4x, 64x, 128x, and 265x diluted extract. The samples 8x, 16x, and 32x had concentrations of 4.62, 6.77, and 2.28 ng/mL respectively, where 2.26ng/mL is closest to the expected halving concentration for each dilution. The last three values for 64x, 128x, and 256x, might indicate that the lower detection limit with the low range RiboGreen RNA quantification assay was reached.*

In conclusion, NP components in the supernatant of the washings during NP formulation increased RiboGreen fluorescence, which needs to be considered for obtaining reliable standard curves. None of the tested mRNA batch supernatants showed a consistent halving of concentration with dilution, indicating unreliable quantification under those conditions. Additionally, FGmRNA could not be separated from contaminants using a 100kDa Amicon filter, as it remained in the retentate. Finally, mRNA extraction from NPs before RNA quantification, showed the most potential for reliable results and accurate encapsulation efficiency determination.

### 3.3.3 Successful transfection of RAW macrophages with GFP-mRNA NPs

To assess whether the mRNA remained intact after NP formulation, RAW macrophages were transfected for 24 h with mRNA-loaded NPs and observed by fluorescence microscopy at 24- and 48-hours post-treatment. Additionally, flow cytometry was used to quantify transfection efficiency.

After treatment with batches WTG08, WTG22, WTG23, and WTG24, RAW macrophages were imaged at 24 and 48 hours, with the images of the 48-hour condition shown in Figure 14. Batch WTG08, E-NPs, was used as a negative control, WTG22 contained 10 µg mRNA, WTG23 contained 10 µg L-mRNA, and WTG24 contained 10 µg mRNA/PEI complex in a 1:0.798 w/w ratio. All samples were imaged in FITC, Rhod, and DAPI channels, corresponding respectively to GFP expression, Cy3 labelling of mRNA, and an autofluorescence check. Remaining images for the 24-hour timepoint and the DAPI channel are included in the appendix Figure S14 and S15. As expected, the E-NPs (WTG08) showed no fluorescence in both the 24- and 48-hours condition in the GFP and Cy3 channels, indicating there was no background signal caused by E-NPs (Figure 14A and S15). Treatment with mRNA-loaded NPs (batch WTG22) led to detection of only one GFP-positive cell, which also contained Cy3 signal in the 48-h condition (Figure 14B). The batch containing mRNA/PEI complex (WTG24) resulted in increased number of GFP-expressing cells, where both high and low GFP-expressing cells were present compared to WTG22 (Figure 14C). Interestingly, for the Cy3-labelled mRNA NPs (WTG23), almost all cells contained Cy3 fluorescence in the Rhod channel, but no GFP expression was observed (Figure 14D). This confirms successful NP uptake but suggests that Cy3 labelling may interfere with GFP translation or lack of lysosomal escape. In conclusion, both batches without PEI complexing, mRNA and L-mRNA, exhibited no GFP expression, in contrast to the mRNA/PEI batch. Furthermore, Cy3 labelling can be used to track NP uptake, however it might interfere with GFP expression.

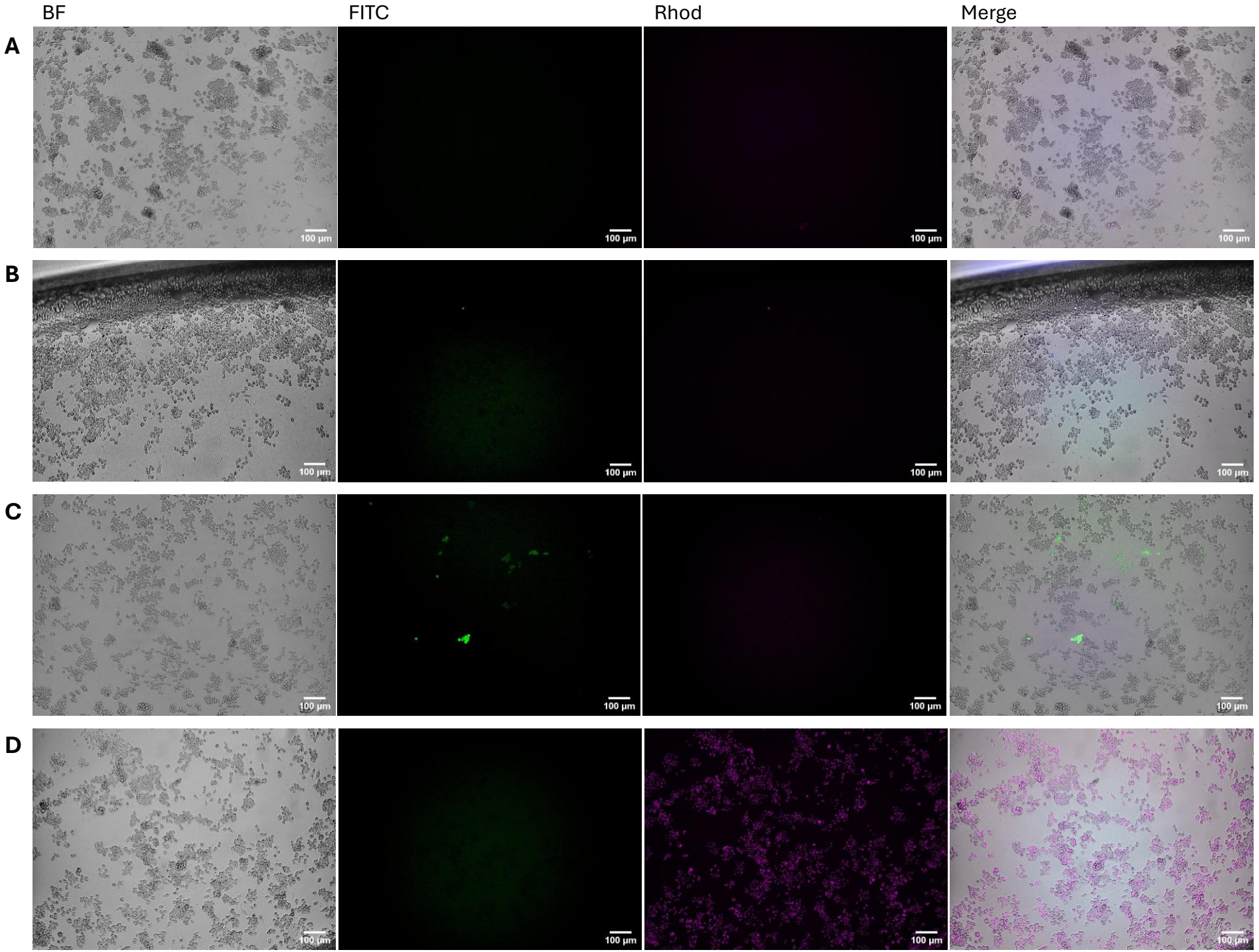


***Figure 14: Fluorescent imaging of GFP transfection of RAW macrophages with mRNA NP batches.*** *RAW macrophages were incubated for 24h with 1,2mg of NPs per well and imaged 48h post treatment.* ***A:*** *E-NPs (batch WTG08) as control, no fluorescence was observed in the chosen channels.* ***B:*** *mRNA NPs (batch WTG22), a single cell showed fluorescence in both the FITC and Rhod channel indicating GFP and Cy3 presence.* ***C:*** *1:0.798 w/w mRNA/PEI (batch WTG24), multiple green-fluorescent cells were observed at different intensities, while no Cy3 fluorescence was present.* ***D:*** *L-mRNA (batch WTG23), none of the observed cells showed GFP fluorescence, however, close to all cells contained Cy3 fluorescence in the Rhod channel. Images were adjusted with FIJI ImageJ*

Some of batches used for the fluorescence microscopy experiments (Figure 14 above), were also analysed by flow cytometry, including L-mRNA (WTG23) in green and mRNA/PEI ratio 1:0.798 w/w (WTG24) in yellow (Figure 15). Additionally, two mRNA/PEI nanoparticle batches were tested: WTG25 (mRNA/PEI 1:1.329 w/w) in pink, and WTG26 (L-mRNA/PEI 1:0.798 w/w) in dark blue.
The percentage of GFP-positive cells was determined by excluding almost all events of the control with a gate in FlowJo as described in the materials and methods (Figure 4). A significant increase in GFP-positive cells was observed only for the mRNA/PEI (1:0.798) NPs, with 0.84% of the cells showing GFP positivity, compared to the controls (Figure 15A). However, the percent change in GFP median fluorescent intensity (MFI) compared to the untreated control showed an increase in fluorescent signal measured (Figure 15B). This shift in MFI was the strongest for mRNA/PEI-loaded NPs with a w/w ratio of 1:1.329, in pink, with a significant increase of 25.9 %. For the other mRNA NP batches, a non-significant increase of 11,2 and 17,6 % was observed, indicating that cells did express low levels of GFP. However, these low levels of GFP expression were apparently insufficient for obtaining GFP-positive cells. Cell viability was not affected by 24 hours of transfection with NPs, as no differences were observed between groups (Figure 15C). Batches containing L-mRNA, WTG23 in green and WTG26 in dark blue, showed a clear increase in Cy3 fluorescence for the whole population, confirming NP uptake by the cells (Figure 15D).
This shift in Cy3 fluorescence observed in the entire population of batch WTG23 is consistent with the fluorescence microscopy results, where nearly all cells showed Cy3 signal (Figure 14D). Additionally, WTG23 showed no significant increase in GFP-positive cells, similar to the fluorescence microscopy experiment. However, for all batch there was an increase in percent change, suggesting that GFP expression in most RAW macrophages may be below the threshold in fluorescence microscopy.

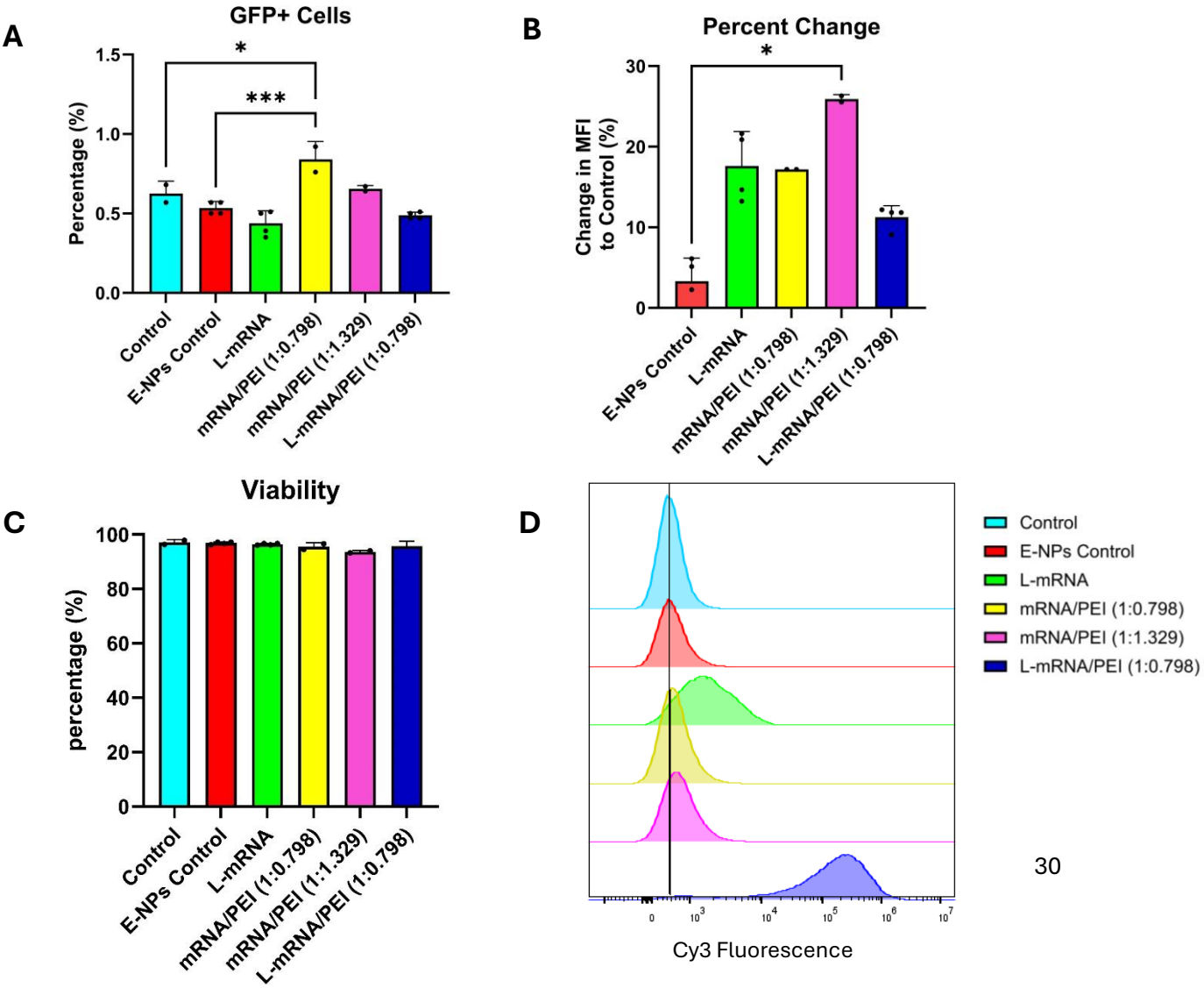

***Figure 15: Flow cytometry data of transfection with commercial mRNA NPs (WTG23-26 & WTG30). A:*** *The percentage of GFP positive cells, compared to the untreated control (0.63 %) there were no visible differences in percentage GFP positive cells, with 0.84 % for mRNA/PEI (1:6) NPs in yellow being the highest. No significance between groups was seen* ***B:*** *percent change of MFI of GFP compared to the untreated control, an increase of 11-26 % in MFI was seen for mRNA encapsulated NPs.* ***C:*** *The viability of cells after transfection, no significant differences were observed* ***D:*** *Cy3 fluorescence of the different tested batches, for L-mRNA NPs in green a clear positive shift was visible. For L-mRNA/PEI NPs in dark blue a big shift in fluorescence was observed, where almost the whole population contained was Cy3 positive. Statistical analysis was performed using a one-way ANOVA followed by Tukey's post-hoc test with statistical significance defined as $p < 0.05$ (*), $p < 0.01$ (**), and $p < 0.001$ (***).*

In the second experiment, cells were incubated either 24- or 48-hours post-transfection, and batches WTG30-34 were tested. For clarity reasons significance between some of the groups is not shown in Figure 16, however a full overview is included in the appendix Figure S8. All batches, except the E-NPs, contained FGmRNA as well as L-FGmRNA (Figure 16). Batch WTG34, labelled as "6x mRNA/PEI" (shown in pink in Figure 16), was formulated with six times the amount of mRNA/PEI in the first water phase compared to the other batches. The percentage of GFP-positive cells increased significantly from 0.4% (standard mRNA/PEI) to 2.0% (6x mRNA/PEI) when increasing the amount of mRNA during formulation, as seen in Figure 16A (green and pink respectively). This improvement was also reflected in the significant precent change in GFP MFI when compared to the E-NP control (Figure 16B). At 24 hours, the standard FGmRNA/PEI NPs showed a 13.7% increase in MFI, while the 6x FGmRNA NPs showed a 51 % increase. However, for all tested mRNA NP batches, the percent change in GFP MFI decreased significantly when comparing the 24- and 48-hour timepoints, suggesting that transfection efficiency and GFP expression peaked before 48-hour post-treatment. Cell viability remained above 90 % for all NP-treated groups, except for the 6x mRNA/PEI NPs where viability dropped significantly to 87.3 % after 24-hour treatment compared to the E-NP control and the standard FGmRNA/PEI NPs (Figure 16C). This suggests a minor increase in cytotoxicity at higher mRNA/PEI concentrations. Interestingly, cells transfected with the FGmRNA or FGmRNA/PEI-loaded NPs, represented in green, orange, and pink (Figure 16C), showed two distinctive in Cy3 populations in flow cytometry. In contrast, cells transfected with L-mRNA NPs, shown in light green and dark blue in Figure 15D, displayed only one clearly shifted Cy3-positive population. In conclusion, both FGmRNA and FGmRNA/PEI NP batches significantly increased the MFI percent change in GFP compared to the E-NP control. However, all tested mRNA NP batches showed reduced GFP expression at 48 hours incubation compared to 24 hours, Additionally, increasing the amount of encapsulated FGmRNA/PEI by sixfold more than quadrupled the percentage of GFP-positive cells from 0.4% to 2.0% and increased the MFI percent change from 13.7% to 51.0%. These findings indicate that increasing the mRNA payload significantly enhances transfection efficiency, although higher concentrations may slightly reduce cell viability.

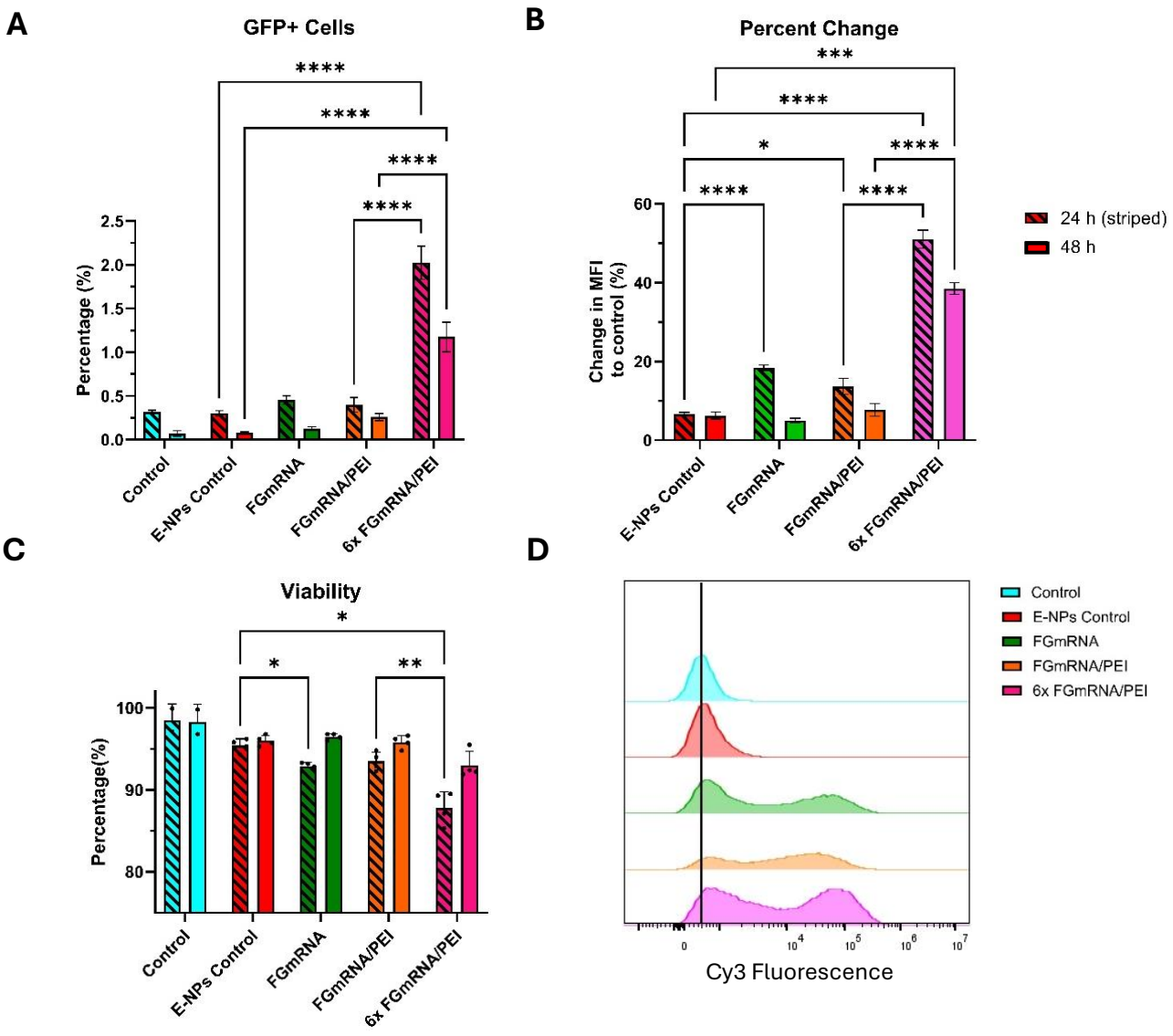


***Figure 16: Flow cytometry data of the 24- and 48-hours transfection groups with FGmRNA NP batches (WTG30-32 & WTG34). A****: The percentage of GFP positive cells, after 24 hours the 6x FGmRNA/PEI NPs showed a significant increase in percentage of GFP positive cells compared to the control and standard FGmRNA/PEI NPs, with 2.0 % compared to 0.4 %. However, for the 48-hour timepoint the percentage of GFP positive cells decreased significantly for each tested batch compared to 24-hour timepoint.* ***B:*** *The percent change of MFI in GFP in mRNA NP batches compared to the untreated cells in blue. There was a significant increase in percent change for all tested FGmRNA NP batches compared to the E-NP control. The 6x FGmRNA/PEI NPs group showed the highest increase in MFI with 51% and 38% for 24 and 48 hours respectively. The percent change decreased significantly for all 48-hour NP treated groups compared to the corresponding 24-hour groups.* ***C:*** *The viability of RAW macrophages after transfection, a decrease in viability can be seen for all treatment groups with 6x FGmRNA/PEI NPs had the lowest viability of 87,8 % and 93 % for 24 and 48 hours respectively.* ***D:*** *The Cy3 fluorescence of the 24-hour transfection condition, all FGmRNA NP treated groups showed a small fluorescent shifted population compared to the untreated control in blue, alongside a clear Cy3-positive population. Statistical analysis was performed using an two-way ANOVA followed by Tukey's post-hoc test with statistical significance defined as $p < 0.05$ (*), $p < 0.01$ (**), $p < 0.001$ (***), and $p < 0.0001$ (****).*

# 4. Discussion

This master's thesis project was carried out in the context of a larger collaborative consortium effort known as TRACER, which aims to develop a gene therapy for sickle cell disease by delivering genetic modification tools, specifically a base editor, into target cells using PLGA nanoparticles (NPs). Within this broader framework, the goal of this thesis was to develop and optimize a PLGA-based delivery platform capable of efficiently entrapping and delivering nucleic acid cargo, with a particular focus on mRNA encapsulation. While the long-term objective of the TRACER project is to apply this platform for therapeutic genome editing in sickle cell disease, this study focused on validating the platform by using GFP-mRNA as a model to assess transfection efficiency and nanoparticle performance.

This thesis demonstrates that GFP-mRNA-loaded PLGA NPs can effectively transfect RAW 264.7 macrophages, which results in low level GFP expression. Initially, RNP complexes were successfully encapsulated into PLGA NPs, with an IEE of 58%, confirmed by BCA assay and Western blot. These RNP-loaded NPs were tested on erythroid progenitor cells by the collaborator, but the treatment did not result in effective transfection. Since only Western blotting and BCA assays were performed, the integrity of the RNP complex after NP formulation remains uncertain. Standard curves for the BCA assay were prepared with contaminant levels matching those of the tested samples to improve accuracy. This approach follows previous studies demonstrating the impact of NP components on assay outcomes [33]. The Western blot of the BE stock and the RNP NPs showed multiple bands, which lessen in intensity after dilution. Given that the base editor was received as a purified protein from our collaborator, these bands likely represent degradation and aggregation products [34]. This suggests that the protein may have been affected either during handling prior to encapsulation or by sonication during formulation. While Cruz et al. 2021 demonstrated successful editing in erythroid cells, indicating that the protein can survive sonication. Furthermore, while not a base editor, CRISPR protein and CRISPR RNP complexes have been shown to remain fully functional after 20 freeze-thaw cycles [35]. They are stable for up to 2 months at 4°C and viable for up to 3 days at RT. This suggests that the handling of the BE during NP formulation may not be the cause of the negative transfection results, given the similarities between BE and CRISPR RNPs. Alternatively, the sgRNA component could have been damaged or separated from the protein due to shear forces during sonication [24], though this was not investigated further in this research. The only other study identified that complexed CRISPR/Cas9 with sgRNA prior to PLGA nanoparticle formulation, used homogenization rather than sonication in the double emulsion solvent evaporation method [18].

On the other hand, GFP-mRNA NPs demonstrated the ability to transfect RAW macrophages, as seen with fluorescence microscopy and flow cytometry. Despite this promising result, several challenges in mRNA NP formulation, quantification, and transfection efficiency remain, for instance mRNA quantification with the RiboGreen still needs optimization. Neither the indirect encapsulation efficiency (via supernatant measurements) nor the direct encapsulation efficiency (via mRNA extraction) provided consistent results. Standard curves indicated that contaminants in the supernatant significantly increase RiboGreen fluorescence, likely interfering with sample measurements as well. Efforts to reduce this interference, such as diluting the supernatant or filtering it through a 100 kDa Amicon membrane, were unsuccessful. Additionally, FGmRNA (~1400 bp) did not pass through the filter, remaining in the retentate. As a result, filtration cannot be used to remove high-molecular-weight contaminants in this context. Given these limitations, direct mRNA quantification via extraction from PLGA NPs appears to be the most feasible

approach. Several previous studies determine the DEE by extracting RNA from PLGA NPs, similar to the method used here, with one key difference: chloroform was used to dissolve the NPs instead of DCM [29, 36, 37]. Due to time constraints, only one extraction attempt was performed in this study, so further optimization of the protocol is necessary.
Moreover, the percentage of GFP-positive cells remains low, with a maximum of 2 %. However, a significant shift in the mean fluorescence intensity (MFI) and a 51 % increase in percentage change were observed for the most optimal condition when compared to the untreated control. This shift in MFI suggests an increase in GFP fluorescence, indicating the presence of low-level GFP expression. For macrophages to be classified as GFP-positive, mRNA uptake and subsequent release from the NPs must be sufficient to exceed the fluorescence threshold of the negative population. The low encapsulation of mRNA in the batches likely contributes to the minimal expression observed. Increasing the amount of mRNA in the first aqueous phase, as done for the 6x FGmRNA/PEI NP batch, resulted in a fourfold increase in the percentage of GFP-positive macrophages. In a comparable study by Sharifnia et al. (2018), where 4 mg of synthetic GFP-mRNA was encapsulated in 25 mg of PLGA (over 60 times the amount used here), a transfection efficiency of 70.2% was achieved after 48 hours. However, in their study, PEI was also incorporated into the organic PLGA phase during formulation to enhance mRNA release and encapsulation. The addition of PEI to the organic phase during formulation is supposed to help with endosomal escape [21], which could also contribute to the difference in transfection efficiency. Additionally, only 30 seconds of sonication were used to form the first emulsion, which likely reduced mechanical shear stress and helped preserve mRNA integrity [32]. In this study, the effects of sonication on mRNA integrity could not be assessed, as conclusions could not be drawn from a single attempt to visualize the mRNA on an RNA gel (Appendix Figure S4). The signal observed in the well indicates that the mRNA did not migrate, suggesting it remained trapped within the NPs, as PLGA NPs are not typically visible in gel electrophoresis [38]. To properly assess mRNA integrity, the nanoparticles would need to be disrupted, and the mRNA extracted and released from PEI, for example, using an SDS solution [27, 38].

After optimizing GFP-mRNA transfection through improved PLGA NP formulation in RAW macrophages, it is possible to extend this approach to other protein-encoding mRNAs. This makes it theoretically feasible to encapsulate a wide range of protein and genetic tools for various applications, provided that the mRNA is not fragmented by sonication. Longer mRNA strands are more likely to be prone to fragmentation than shorter ones, due to the greater number of potential hydrolysis sites [39] and increased susceptibility to mechanical shear stress [32]. While lipid nanoparticles (LNPs) are the most commonly used mRNA delivery vector, PLGA NPs offer significant advantages, including enhanced stability and ease of modification [17]. LNPs are more susceptible to environmental changes than polymeric nanoparticles, which can negatively impact their shelf life and stability [40]. Depending on the application, PLGA NPs may be the preferred mRNA vector for in vivo use. For example, PLGA NPs are known to predominantly localize in the spleen and bone marrow after intravenous injection in mice [41], regions where erythroid progenitor cells are located [6], the target cells for sickle cell disease. Although erythroid progenitor cells exhibit some phagocytic activity, especially during inflammation, this is not as pronounced as the high phagocytic activity observed in RAW 264.7 macrophages [42]. Therefore, cellular uptake of PLGA NPs can be further optimized for specific targets through surface modifications, such as polyethylene glycol (PEG). PEG can improve nanoparticle stability and biocompatibility, and also serves as a linker to conjugate targeting molecules, such as antibodies, folate, or transferrin, to enhance cellular uptake [1]. However, the use of PEI in PLGA

NP formulation to enhance encapsulation efficiency and facilitate endosomal escape may limit applications to in vitro use, due to its associated cytotoxicity, as observed in previous studies [43].

Although this represents a promising initial result, further optimization of nanoparticle (NP) formulation could enhance transfection efficiency. First, for protein delivery, a smaller first aqueous phase has been shown to increase EE; however, Alanazi et al. (2022) demonstrated that a larger first aqueous phase improved microRNA encapsulation. Optimal phase ratios during NP formulation for mRNA encapsulation may differ from those required for optimal protein encapsulation. Second, the incorporation of PEI into the organic phase during PLGA NP formulation has been reported to enhance mRNA encapsulation and facilitate mRNA release [27]. The effects of the addition of PEI, in the organic phase as well as mRNA complexing, on endosomal escape could be studied by visualisation of co-localisation of L-mRNA-loaded NPs and a life staining lysotracker using confocal microscopy. Finally, if sonication-induced mechanical shear stress impacts mRNA integrity during formulation of the first emulsion, reducing the sonication time may mitigate this effect [27]. The encapsulation optimizations can be validated through an optimized RiboGreen RNA quantification protocol combined with mRNA extraction, paired with RNA-integrity assessment via gel electrophoresis [27]. Subsequent experiments aimed at increasing transfection efficiency should include the formulation of BE-mRNA- and sgRNA-loaded PLGA NPs, followed by evaluation of gene editing capabilities in erythroid progenitor cells.

# Conclusion

In this study, we aimed to investigate the feasibility of encapsulating ribonucleoprotein (RNP) complexes in PLGA nanoparticles (NPs) and to evaluate the impact of the double emulsion solvent evaporation method with sonication on both the stability of the RNP complexes and the integrity of the mRNA. To achieve this, RNP complex-, BSA-, and mRNA-loaded PLGA NPs were formulated, characterized, encapsulation efficiencies quantified, and mRNA transfection capabilities assessed. While RNP complexes were successfully encapsulated, the RNP-loaded NPs did not induce the desired genetic modification in erythroid progenitor cells. In contrast, GFP-mRNA-loaded NPs successfully transfected RAW 264.7 macrophages, confirming mRNA encapsulation, though quantification with the current methods was not achieved. furthermore, the observed GFP expression indicates intact mRNA and suggests that it can survive sonication, even though this could not be confirmed with gel electrophoresis.
Future studies should focus on optimizing NP formulation to enhance mRNA encapsulation and improve endosomal escape. Additionally, more accurate quantification methods for encapsulation efficiency, an assessment of mRNA integrity post-formulation, and an analysis of endosomal escape mechanisms should be incorporated to better understand the transfection efficiency of these NPs. This prove of concept demonstrates the potential of protein-encoding mRNA-loaded NPs as versatile delivery vectors for genetic modification and gene therapy.

# Acknowledgements

First and foremost, I would like to express my sincere gratitude to Alvja Mali and Mangala Srinivas for their great supervision throughout this project. Their guidance in the lab, as well as their support during meetings, kept me motivated and positive.
Next, I would like to extend my appreciation to the collaborators of the larger TRACER consortium, with special thanks to Memnia Vasiliou for providing the ABE and sgRNA used in NP formulation, as well as for testing the RNP-loaded NPs on their cell line.
I would also like to thank Albert Ngalle Loth, also known as the "French Guy," for generously supplying the purified GFP-mRNA (FGmRNA) used in both NP formulation and testing.
I am deeply grateful to the staff and technicians at CBI, particularly Edwin, Youri, Mojtaba, Robbin, and Koen, for their support with technical challenges and questions beyond my expertise. I also wish to thank Maria from HMI for her assistance and guidance.
Lastly, I would like to thank the students who provided feedback during the thesis rings. You and my upstairs neighbour Janne of HMI made this experience much more enjoyable.

# References


1. Sahu, K.K., et al., *Non-viral nucleic acid delivery approach: A boon for state-of-the-art gene delivery.* Journal of Drug Delivery Science and Technology, 2023. **80**: p. 104152.
2. Amberger, J.S., et al., *OMIM.org: leveraging knowledge across phenotype–gene relationships.* Nucleic Acids Research, 2018. **47**(D1): p. D1038-D1043.
3. Kolanu, N.D., *CRISPR-Cas9 Gene Editing: Curing Genetic Diseases by Inherited Epigenetic Modifications.* Glob Med Genet, 2024. **11**(1): p. 113-122.
4. Li, T., et al., *CRISPR/Cas9 therapeutics: progress and prospects.* Signal Transduction and Targeted Therapy, 2023. **8**(1): p. 36.
5. Doudna, J.A. and E. Charpentier, *The new frontier of genome engineering with CRISPR-Cas9.* Science, 2014. **346**(6213): p. 1258096.
6. Dzierzak, E. and S. Philipsen, *Erythropoiesis: development and differentiation.* Cold Spring Harb Perspect Med, 2013. **3**(4): p. a011601.
7. Kantor, A., M.E. McClements, and R.E. MacLaren, *CRISPR-Cas9 DNA Base-Editing and Prime-Editing.* Int J Mol Sci, 2020. **21**(17).
8. Newby, G.A., et al., *Base editing of haematopoietic stem cells rescues sickle cell disease in mice.* Nature, 2021. **595**(7866): p. 295-302.
9. Wang, H.-X., et al., *CRISPR/Cas9-Based Genome Editing for Disease Modeling and Therapy: Challenges and Opportunities for Nonviral Delivery.* Chemical Reviews, 2017. **117**(15): p. 9874-9906.
10. Kim, S., et al., *Highly efficient RNA-guided genome editing in human cells via delivery of purified Cas9 ribonucleoproteins.* Genome Research, 2014. **24**(6): p. 1012-1019.
11. Yin, H., et al., *Non-viral vectors for gene-based therapy.* Nature Reviews Genetics, 2014. **15**(8): p. 541-555.
12. University, U. *"Failed" experiment with DNA scissors turns out to be cut out for publication after all*. 2024.
13. Hadianamrei, R. and X. Zhao, *Current state of the art in peptide-based gene delivery.* Journal of Controlled Release, 2022. **343**: p. 600-619.
14. Nayak, S. and R.W. Herzog, *Progress and prospects: immune responses to viral vectors.* Gene Ther, 2010. **17**(3): p. 295-304.
15. Lifen Huang, J.H., Junbin Huang, Hongman Xue, Zhiqing Liang, and J.W.a.C. Chen, *Nanomedicine – a promising therapy for hematological malignancies.* Royal society of chemistry, 2020.
16. Krhač Levačić, A., et al., *Dynamic mRNA polyplexes benefit from bioreducible cleavage sites for in vitro and in vivo transfer.* Journal of Controlled Release, 2021. **339**: p. 27-40.
17. Li, X., et al., *Nanoparticle technology for mRNA: Delivery strategy, clinical application and developmental landscape.* Theranostics, 2024. **14**(2): p. 738-760.
18. Srivastav, A., et al., *Efficiency of Chitosan-Coated PLGA Nanocarriers for Cellular Delivery of siRNA and CRISPR/Cas9 Complex.* Journal of Pharmaceutical Innovation, 2022. **17**(1): p. 180-193.
19. Bulcha, J.T., et al., *Viral vector platforms within the gene therapy landscape.* Signal Transduction and Targeted Therapy, 2021. **6**(1): p. 53.
20. Chatterjee, S., et al., *Endosomal escape: A bottleneck for LNP-mediated therapeutics.* Proceedings of the National Academy of Sciences, 2024. **121**(11): p. e2307800120.

21. Wang, Y., et al., *Advancing endosomal escape of polymeric nanoparticles: towards improved intracellular delivery.* Materials Horizons, 2025.
22. Dördelmann, G., et al., *Calcium phosphate increases the encapsulation efficiency of hydrophilic drugs (proteins, nucleic acids) into poly(d,l-lactide-co-glycolide acid) nanoparticles for intracellular delivery.* Journal of Materials Chemistry B, 2014. **2**(41): p. 7250-7259.
23. Choi, J.-S., K. Seo, and J.-W. Yoo, *Recent advances in PLGA particulate systems for drug delivery.* Journal of Pharmaceutical Investigation, 2012. **42**(3): p. 155-163.
24. López-Royo, T., et al., *Encapsulation of Large-Size Plasmids in PLGA Nanoparticles for Gene Editing: Comparison of Three Different Synthesis Methods.* Nanomaterials (Basel), 2021. **11**(10).
25. Español, L., et al., *Dual encapsulation of hydrophobic and hydrophilic drugs in PLGA nanoparticles by a single-step method: drug delivery and cytotoxicity assays.* RSC Advances, 2016. **6**(112): p. 111060-111069.
26. Gavini, E., et al., *PLGA microspheres for the ocular delivery of a peptide drug, vancomycin using emulsification/spray-drying as the preparation method: in vitro/in vivo studies.* European Journal of Pharmaceutics and Biopharmaceutics, 2004. **57**(2): p. 207-212.
27. Sharifnia, Z., et al., *In-vitro Transcribed mRNA Delivery Using PLGA/PEI Nanoparticles into Human Monocyte-derived Dendritic Cells.* Iran J Pharm Res, 2019. **18**(4): p. 1659-1675.
28. Cruz, L.J., et al., *PLGA-Nanoparticles for Intracellular Delivery of the CRISPR-Complex to Elevate Fetal Globin Expression in Erythroid Cells.* Biomaterials, 2021. **268**: p. 120580.
29. Cun, D., et al., *High loading efficiency and sustained release of siRNA encapsulated in PLGA nanoparticles: Quality by design optimization and characterization.* European Journal of Pharmaceutics and Biopharmaceutics, 2011. **77**(1): p. 26-35.
30. Wightman, L., et al., *Different behavior of branched and linear polyethylenimine for gene delivery in vitro and in vivo.* J Gene Med, 2001. **3**(4): p. 362-72.
31. Kafil, V. and Y. Omidi, *Cytotoxic impacts of linear and branched polyethylenimine nanostructures in a431 cells.* Bioimpacts, 2011. **1**(1): p. 23-30.
32. Lokras, A., et al., *Simultaneous quantification of multiple RNA cargos co-loaded into nanoparticle-based delivery systems.* International Journal of Pharmaceutics, 2022. **626**: p. 122171.
33. Clerici, M., et al., *Pitfalls of Accurate Protein Determination inside PLGA Nanoparticles Using the Micro BCA Assay.* Proceedings, 2021. **78**(1): p. 28.
34. Bio-Rad. *Protein Band Size and Pattern Problems*.
35. Spencer, N.Y., A. Jacobi, and R. N. *Stability of CRISPR reagents under different freezing, storage, and thawing conditions*. 2020.
36. McKiernan, P.J., et al., *Knockdown of Gene Expression in Macrophages by microRNA Mimic-Containing Poly (Lactic-co-glycolic Acid) Microparticles.* Medicines, 2018. **5**(4): p. 133.
37. Jensen, D.K., et al., *Design of an inhalable dry powder formulation of DOTAP-modified PLGA nanoparticles loaded with siRNA.* Journal of Controlled Release, 2012. **157**(1): p. 141-148.

38. Alanazi, J.S., et al., *MicroRNA-539-5p-Loaded PLGA Nanoparticles Grafted with iRGD as a Targeting Treatment for Choroidal Neovascularization.* Pharmaceutics, 2022. **14**(2): p. 243.
39. Leppek, K., et al., *Combinatorial optimization of mRNA structure, stability, and translation for RNA-based therapeutics.* bioRxiv, 2021.
40. Mehta, M., et al., *Lipid-Based Nanoparticles for Drug/Gene Delivery: An Overview of the Production Techniques and Difficulties Encountered in Their Industrial Development.* ACS Mater Au, 2023. **3**(6): p. 600-619.
41. Krekorian, M., et al., *Characterization of Intrinsically Radiolabeled Poly(lactic-co-glycolic acid) Nanoparticles for ex Vivo Autologous Cell Labeling and in Vivo Tracking.* Bioconjugate Chemistry, 2021. **32**(8): p. 1802-1811.
42. Tiwari, A., et al., *Cross-Modal Imaging Reveals Nanoparticle Uptake Dynamics in Hematopoietic Bone Marrow during Inflammation.* ACS Nano, 2024. **18**(9): p. 7098-7113.
43. Pontes, A.P., et al., *A poly(amidoamine)-based polymeric nanoparticle platform for efficient in vivo delivery of mRNA.* Biomaterials Advances, 2024. **156**: p. 213713.

# Appendix

*AI disclosure*

During the thesis AI search engines, GPT and Perplexity, were used for literature research on this topic. However, all papers were read and analysed by the writer and put into own context and wording for the final draft. GPT was further used to improve grammar and sentence structure in case the sentences were not clearly formulated according to feedback. No AI of any kind was used to write entire pieces of text, and no AI-given information was used as a direct source.

***Table S1: Batch information of all made batches*** *(from left to right): Batch name, Content added to the W1 phase, volume of the phases (W1, O, and W2), percentage of PVA used in the W2 phase, amount of PLGA added to the O phase. Besides that, the average values for the zeta potential, size and PDI of DLS measurements of the batch.*

| ***Sample Name*** | ***Entrapped*** | **W1 (µL)** | **O (µL)** | **W2 (µL)** | ***PVA (%)*** | ***PLGA (mg)*** | ***zeta potential (mV)*** | ***size (nm)*** | ***PDI*** |
|---|---|---|---|---|---|---|---|---|---|
| WTG-02 | 149 µg RNP complex | 100 | 700 | 3000 | 1 | 10,3 | -35,4 | 219,8 | 0,12 |
| WTG-03 | E-NPs | 100 | 700 | 3000 | 1 | 10,3 | -39,3 | 228,4 | 0,14 |
| WTG-04 | E-NPs | ? | 3000 | 25500 | 1 | 100,1 | -35,2 | 219,2 | 0,18 |
| WTG-05 | 74 µg RNP complex | 250 | 750 | 3000 | 1 | 10,1 | -29,6 | 253,4 | 0,17 |
| WTG-06 | E-NPs | - | 3000 | 25500 | 2 | 100 | -34,9 | 195,4 | 0,06 |
| WTG-07 | E-NPs | - | 3000 | 25500 | 2 | 100,1 | -35,7 | 209,1 | 0,07 |
| WTG-08 | E-NPs | - | 3000 | 25500 | 2 | 100,8 | -37,7 | 203,1 | 0,04 |
| WTG-09 | 2 mg BSA | 250 | 750 | 3000 | 1 | 10,1 | -37,2 | 207,1 | 0,14 |
| WTG-10 | 5 µg mRNA GFP | 100 | 900 | 3000 | 2 | 10,3 | -32,3 | 205,7 | 0,05 |
| WTG-11 | 100 µg BSA | 250 | 750 | 3000 | 1 | 10 | -40,7 | 219,8 | 0,10 |
| WTG-12 | 100 µg BSA | 100 | 900 | 3000 | 1 | 10,2 | -38,5 | 216,7 | 0,07 |
| WTG-13 | 100 µg BSA | 166 | 833 | 3000 | 1 | 10,2 | -36,2 | 215,9 | 0,07 |
| WTG-14 | 5 µg mRNA/PEI (1:0.798) | 100 | 900 | 3000 | 1 | 10,7 | -39,8 | 222,1 | 0,11 |
| WTG-15 | 5 µg L-mRNA/PEI (1:0.798) | 100 | 900 | 3000 | 1 | 10,1 | -30,6 | 207,8 | 0,10 |
| WTG-16 | 5 µg L-mRNA | 100 | 900 | 3000 | 1 | 10,7 | -41,7 | 212,2 | 0,08 |
| WTG-17 | E-NPs | 200 | 1800 | 6000 | 1 | 20,2 | -36,0 | 194 | 0,09 |

| | | | | | | | | | |
|---|---|---|---|---|---|---|---|---|---|
| WTG-18 | E-NPs | 100 | 900 | 3000 | 1 | 10,3 | | | |
| WTG-19 | E-NPs | 100 | 900 | 3000 | 1 | 10,1 | | | |
| WTG-20 | E-NPs | 100 | 900 | 3000 | 1 | 10,8 | | | |
| WTG-21 | E-NPs | 100 | 900 | 3000 | 1 | 10,2 | | | |
| WTG-22 | 10 µg mRNA | 100 | 900 | 4000 | 2 | 20,1 | -21,7 | 285,9* | 0,39 |
| WTG-23 | 10 µg L-mRNA | 100 | 900 | 4000 | 2 | 20,1 | -21,6 | 231,2* | 0,42 |
| WTG-24 | 10 µg mRNA/PEI (1:0.798) | 100 | 900 | 4000 | 2 | 20 | -24,0 | 183,5* | 0,26 |
| WTG-25 | 10 µg mRNA/PEI (1:1.329) | 100 | 900 | 4000 | 2 | 20,8 | | 247.2* | 0.19 |
| WTG-26 | 10 µg L-mRNA/PEI (1:0.798) | 100 | 900 | 4000 | 2 | 20,9 | -25,6 | 201,6* | 0,38 |
| WTG-27 | E-NPs | 100 | 900 | 3000 | 1 | 20,5 | -33,0 | 225,6 | 0,11 |
| WTG-28 | E-NPs | 100 | 900 | 3000 | 2 | 20,9 | -30,9 | 222,8 | 0,16 |
| WTG-29 | E-NPs | 100 | 900 | 4000 | 2 | 19,9 | -36,8 | 200,2 | 0,09 |
| WTG-30 | E-NPs | 100 | 900 | 4000 | 2 | 30,6 | -35,5 | 203,2 | 0,08 |
| WTG-31 | 10 µg FGmRNA/PEI (1:0.399) +2 ug L-FGmRNA/PEI (1:0.266) | 100 | 900 | 3000 | 2 | 20,6 | -23,6 | 198,6 | 0,09 |
| WTG-32 | 10 µg FGmRNA +1 µg L-FGmRNA | 100 | 900 | 3000 | 2 | 20,3 | -39,9 | 204,4 | 0,10 |
| WTG-33 | 10 µg mRNA/PEI (1:0.399) + 2 µg L-mRNA/PEI (1:0.266) | 100 | 900 | 3000 | 2 | 20,6 | -23,4 | 208,5 | 0,09 |
| WTG-34 | 60 µg FG mRNA/PEI (1:0.399) + 2 µg L-FGmRNA/PEI (1:0.266) | 100 | 900 | 3000 | 2 | 20,6 | -18,1 | 203,3 | 0,11 |
| WTG-35 | 5 µg high labelling density L-FGmRNA | 100 | 900 | 4000 | 2 | 20,8 | -34,7 | 167.1* | 0,56 |
| WTG-36 | 10 µg FGmRNA/PEI (1:0.399) stored | 100 | 900 | 4000 | 2 | 15,5 | -9,8 | 205,1 | 0,14 |
| WTG-37 | 10 µg FGmRNA/PEI (1:0.399) fresh | 100 | 900 | 4000 | 2 | 15,1 | -41,2 | 203,8 | 0,11 |
| WTG-38 | 5 µg mRNA/PEI (1:0.399) | 100 | 900 | 4000 | 2 | 10,9 | -36,5 | 206,3 | 0,15 |

(* = NP size based on size by numbers of data)

***Table S2: Qubit RNA concentration measurements on samples containing E-NPs, BE or both,*** *as validation of the method for determining the RNA concentration of PLGA NP batches encapsulating RNA and the effect of contaminants (PVA, PLGA, and BE) on the outcome of the measurement. The theoretical concentration is based on the RNA stock measurement (162 ng/µL) and the dilutions made during sample preparation of the other conditions.*
*NOTE: RNA used in these measurements and samples is isolated whole genome RNA gifted from Maria (HMI) and not sgRNA.*

| ***Sample name*** | ***Concentration (ng/µL)*** | ***Theoretical conc. (ng/µL)*** |
|---|---|---|
| *E-NPs* | *136* | *-* |
| *RNA stock* | *162* | *162* |
| *RNA + Base Editor* | *71* | *108* |
| *RNA + BE + NPs* | *21,8* | *64,8* |
| *RNA + NPs* | *85,4* | *88* |

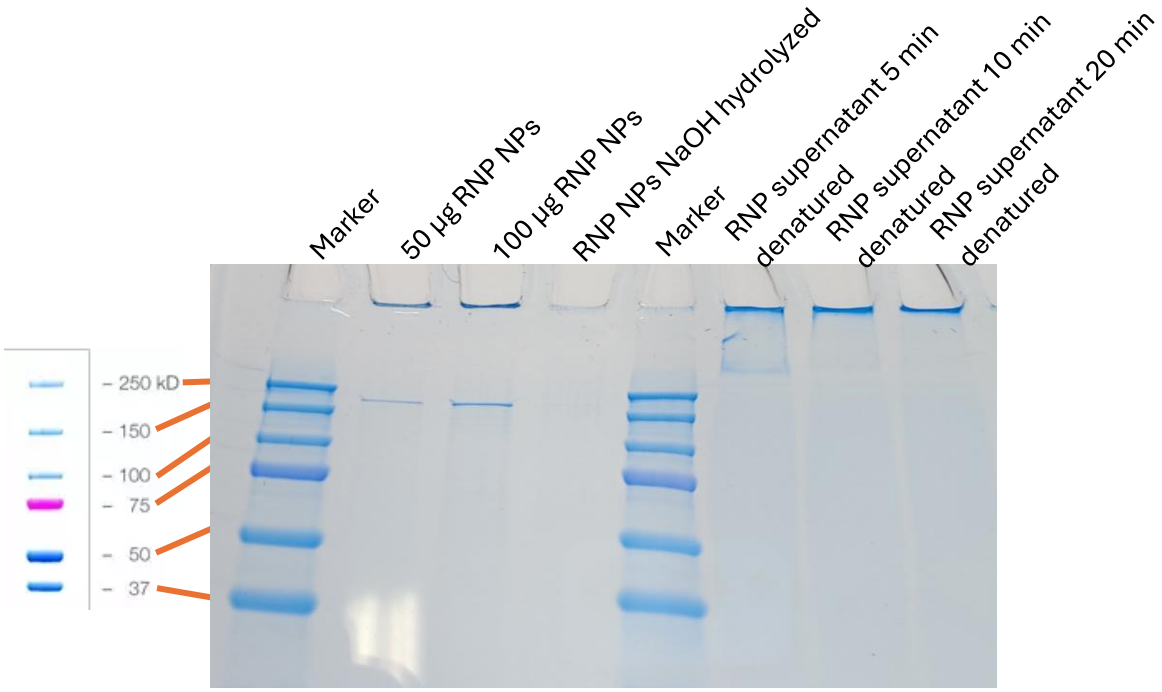


***Figure 17: SDS-PAGE of RNP NPs and RNP supernatant.*** *Lane 2 and 3: RNP NPs were loaded without denaturation at 70 °C. Lane 4: RNP NPs were hydrolysed with NaOH, and protein were precipitated with TCA. Lane 6, 7, and 8: RNP supernatant was denatured in SDS loading dye at 70 °C for 5 min, 10 min or 20 min respectively.*

***Table S3: BCA assay values and IEE of BSA batches***

| **Sample name** | **Measured Conc. in Supernatant (µg /mL)** | **Total amount in supernatant (µg)** | **IEE (%)** | **LC (%)** |
|---|---|---|---|---|
| WTG09 | 345 | 1468.17 | 27 | 10.85 |
| WTG11 | 5.35 | 22.76 | 77 | 1.12 |
| WTG12 | 2.64 | 11.21 | 89 | 1.15 |
| WTG13 | 9.55 | 40.61 | 59 | 0.80 |

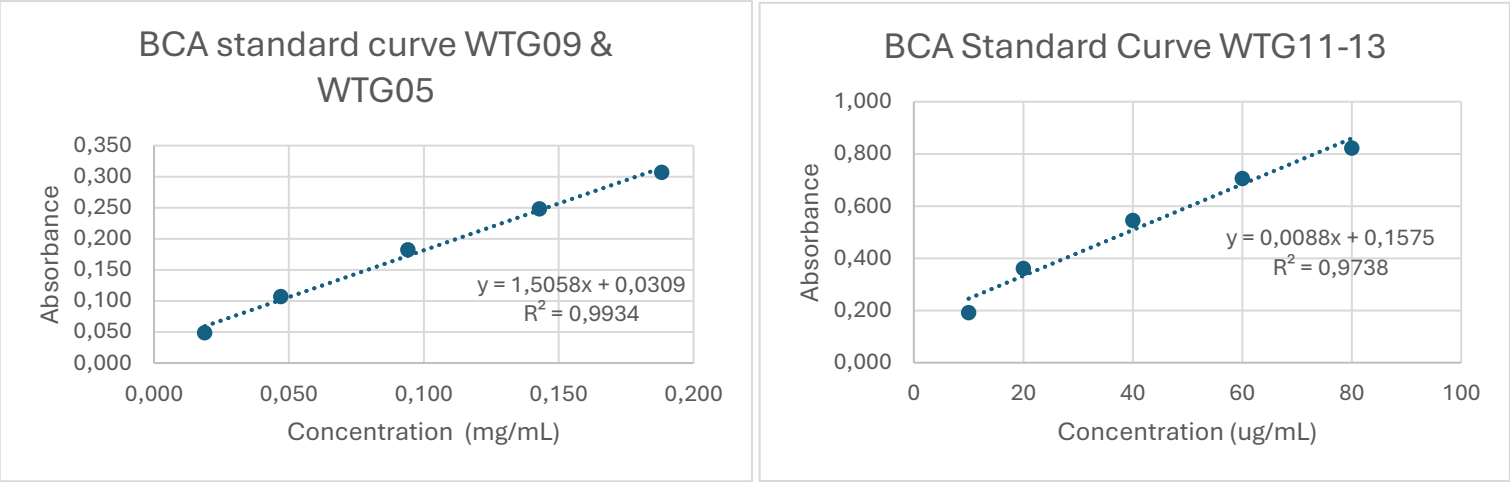


***Figure S2: Standard curves made for the BCA assay of A:*** *the RNP batch WTG05 and BSA batch WTG09 and* ***B:*** *BSA batches WTG11, WTG12, and WTG13. Note the difference in range for A and B on the x-axis.*

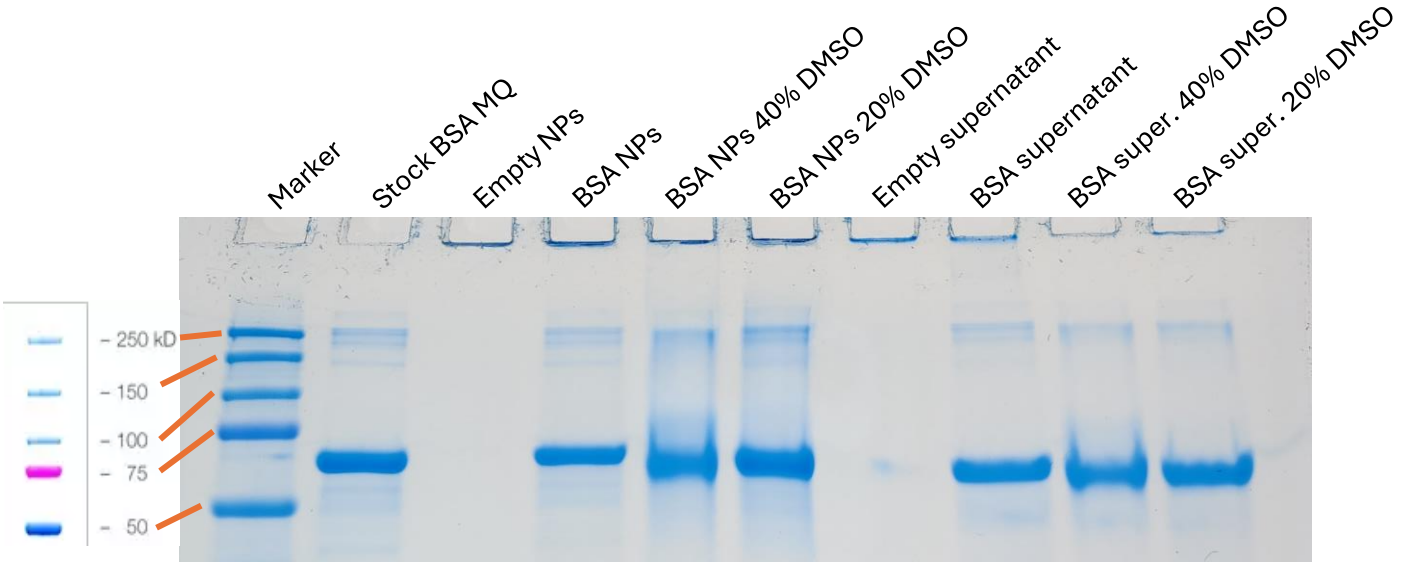


***Figure S3: SDS-PAGE of BSA NPs and supernatant, as well as E NPs***

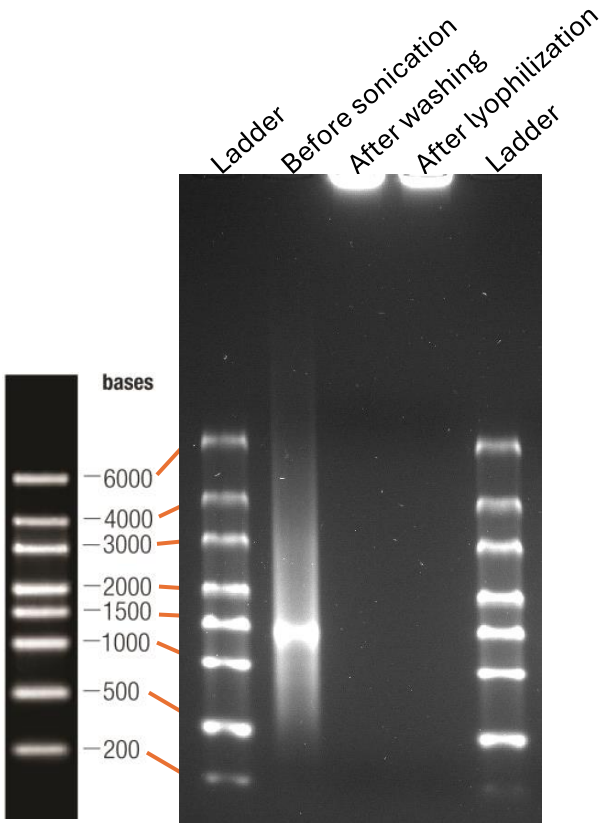


***Figure S4: RNA gel of mRNA during different stages in NP preparation**. Before sonication a sample from the W1 phase, after two washings, and after lyophilization and resuspended in RNase free water was taken and put on the RNA gel.*

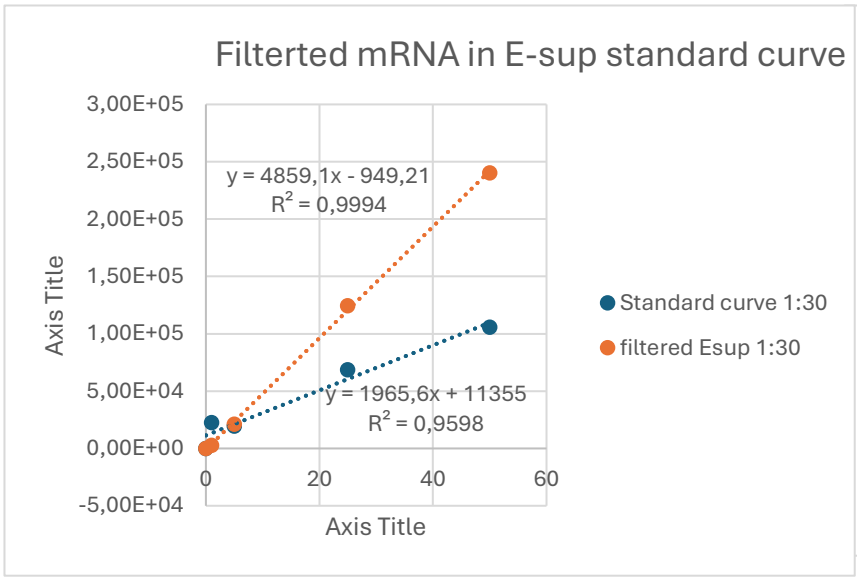


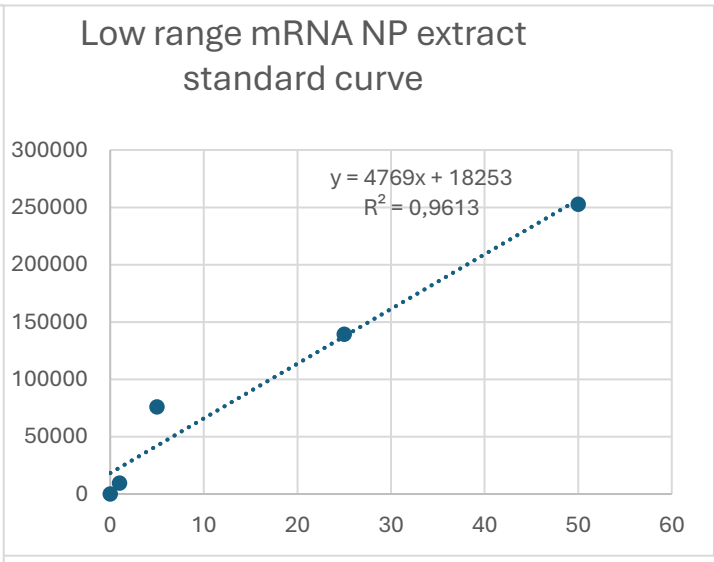


***Figure S5: RNA quantification standard curve of A:** filtered mRNA in E-sup to remove contaminants **and B:** standard curve of extracted E-NP with mRNA**.***

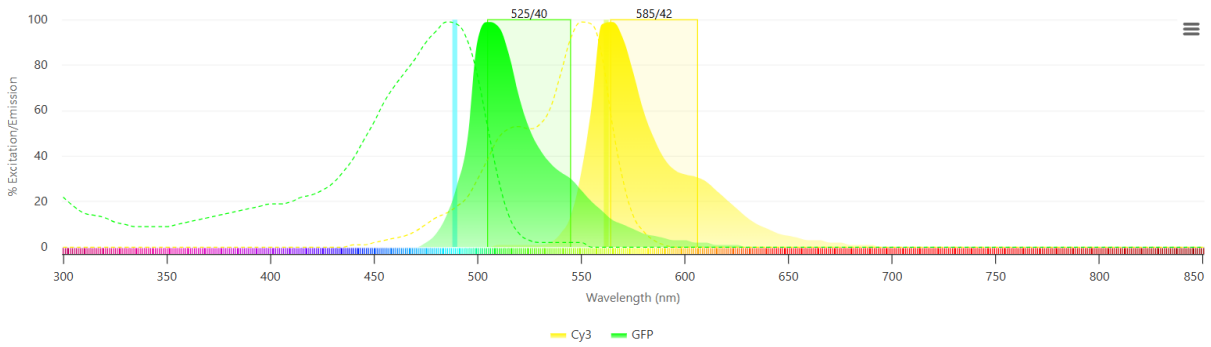


***Figure S6: Emission (full line) and Excitation (dotted line) spectra of GFP (in green) and Cy3 (in yellow) and the excitation laser and filters used to measure fluorescence by Cytoflex LX.***

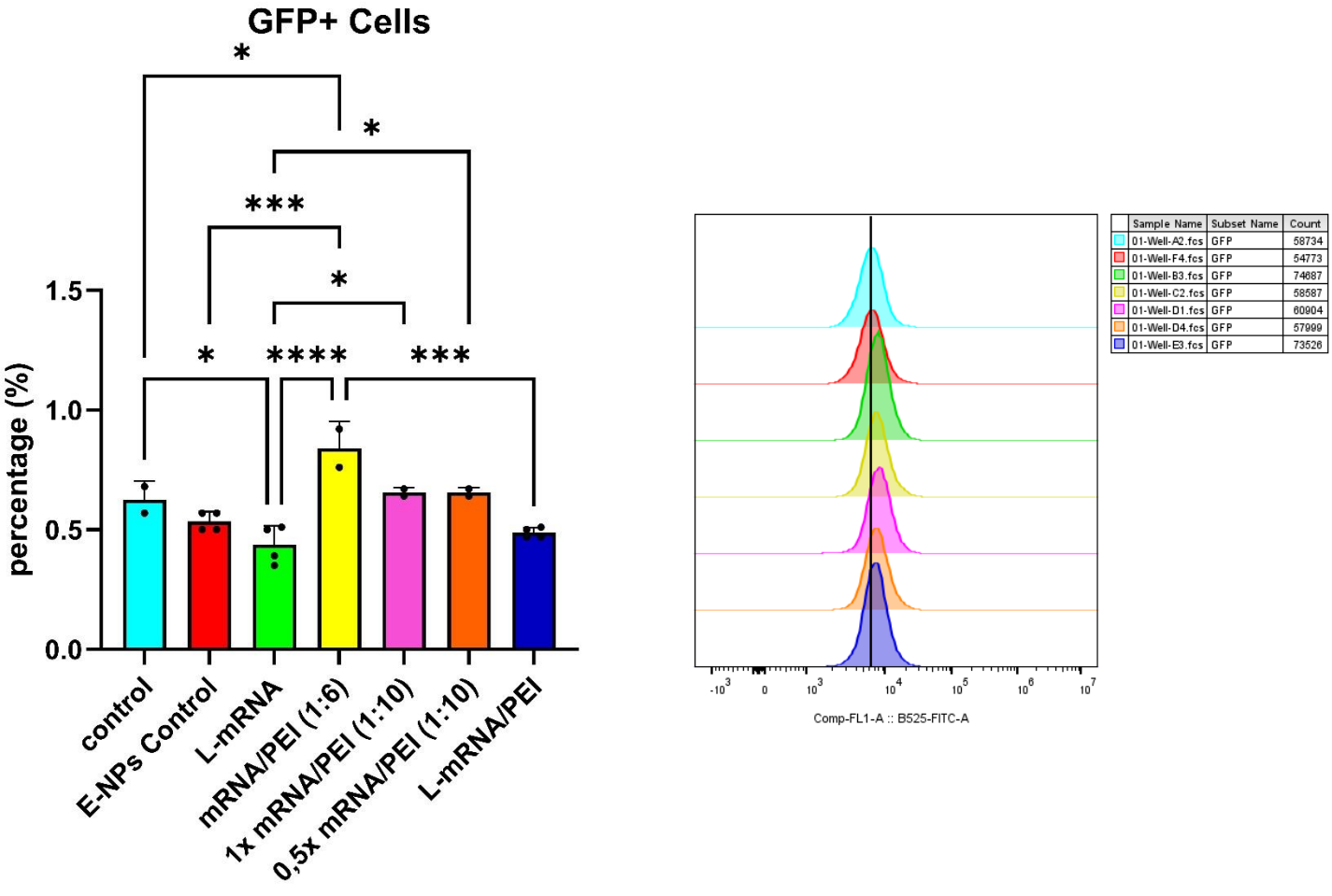


***Figure S7: Complete overview of significant differences between all groups of Figure 15A, and FITC histograms corresponding to the GFP-MFI percent change.*** *Statistical analysis was performed using a one-way ANOVA followed by Tukey's post-hoc test with statistical significance defined as $p < 0.05$ (*), $p < 0.01$ (**), $p < 0.001$ (***), and $p < 0.0001$ (****).*

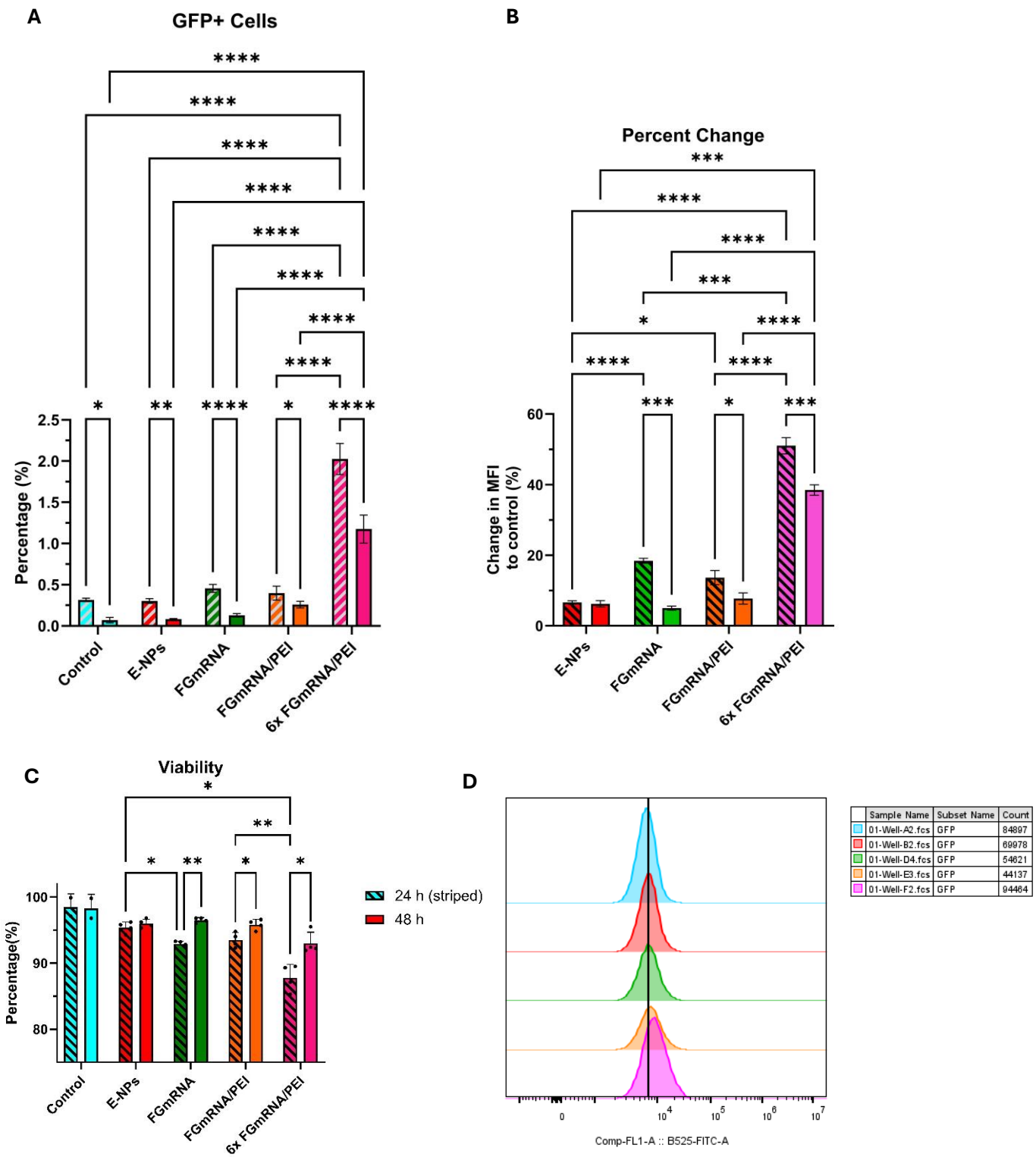


***Figure S8: Complete overview of significant differences between all groups of Figure 16A/B/C, and FITC histograms corresponding to the GFP-MFI percent change.*** *Statistical analysis was performed using a two-way ANOVA followed by Tukey's post-hoc test with statistical significance defined as $p < 0.05$ (*), $p < 0.01$ (**), $p < 0.001$ (***), and $p < 0.0001$ (****).*

| 2way ANOVA<br>Multiple comparisons | | | | | |
|---|---|---|---|---|---|
| | | | | | |
| Compare cell means with others in its row and its column | | | | | |
| | | | | | |
| Number of families | 8 | | | | |
| Number of comparisons per row family | 15 | | | | |
| Number of comparisons per column family | 1 | | | | |
| Alpha | 0.05 | | | | |
| | | | | | |
| **Tukey's multiple comparisons test** | **Mean Diff.** | **95.00% CI of diff.** | **Below threshold?** | **Summary** | **Adjusted P Value** |
| | | | | | |
| 24h | | | | | |
| E-NPs Control vs. FGmRNA | -11.79 | -13.37 to -10.21 | Yes | **** | <0.0001 |
| E-NPs Control vs. FGmRNA/PEI | -7.035 | -12.34 to -1.726 | Yes | * | 0.0230 |
| E-NPs Control vs. mRNA/PEI | -19.48 | -27.22 to -11.73 | Yes | ** | 0.0035 |
| E-NPs Control vs. 6x FGmRNA/PEI | -44.39 | -50.88 to -37.90 | Yes | **** | <0.0001 |
| E-NPs Control vs. 6x FGmRNA/PEI | -44.39 | -50.88 to -37.90 | Yes | **** | <0.0001 |
| FGmRNA vs. FGmRNA/PEI | 4.758 | -2.119 to 11.63 | No | ns | 0.1288 |
| FGmRNA vs. mRNA/PEI | -7.685 | -16.53 to 1.158 | No | ns | 0.0725 |
| FGmRNA vs. 6x FGmRNA/PEI | -32.60 | -40.35 to -24.84 | Yes | *** | 0.0010 |
| FGmRNA vs. 6x FGmRNA/PEI | -32.60 | -40.35 to -24.84 | Yes | *** | 0.0010 |
| FGmRNA/PEI vs. mRNA/PEI | -12.44 | -19.10 to -5.786 | Yes | ** | 0.0086 |
| FGmRNA/PEI vs. 6x FGmRNA/PEI | -37.35 | -42.21 to -32.49 | Yes | **** | <0.0001 |
| FGmRNA/PEI vs. 6x FGmRNA/PEI | -37.35 | -42.21 to -32.49 | Yes | **** | <0.0001 |
| mRNA/PEI vs. 6x FGmRNA/PEI | -24.91 | -30.40 to -19.42 | Yes | *** | 0.0008 |
| mRNA/PEI vs. 6x FGmRNA/PEI | -24.91 | -30.40 to -19.42 | Yes | *** | 0.0008 |
| 6x FGmRNA/PEI vs. 6x FGmRNA/PEI | 0.000 | | | | |
| | | | | | |
| 48h | | | | | |
| E-NPs Control vs. FGmRNA | 1.223 | -2.369 to 4.814 | No | ns | 0.5136 |
| E-NPs Control vs. FGmRNA/PEI | -1.498 | -5.512 to 2.517 | No | ns | 0.4492 |
| E-NPs Control vs. mRNA/PEI | -7.855 | -12.61 to -3.101 | Yes | * | 0.0122 |
| E-NPs Control vs. 6x FGmRNA/PEI | -32.24 | -38.00 to -26.48 | Yes | *** | 0.0003 |
| E-NPs Control vs. 6x FGmRNA/PEI | -32.24 | -38.00 to -26.48 | Yes | *** | 0.0003 |
| FGmRNA vs. FGmRNA/PEI | -2.720 | -6.807 to 1.367 | No | ns | 0.1413 |
| FGmRNA vs. mRNA/PEI | -9.078 | -14.53 to -3.628 | Yes | * | 0.0120 |
| FGmRNA vs. 6x FGmRNA/PEI | -33.46 | -36.37 to -30.56 | Yes | **** | <0.0001 |
| FGmRNA vs. 6x FGmRNA/PEI | -33.46 | -36.37 to -30.56 | Yes | **** | <0.0001 |
| FGmRNA/PEI vs. mRNA/PEI | -6.358 | -13.94 to 1.230 | No | ns | 0.0798 |
| FGmRNA/PEI vs. 6x FGmRNA/PEI | -30.74 | -34.58 to -26.90 | Yes | **** | <0.0001 |
| FGmRNA/PEI vs. 6x FGmRNA/PEI | -30.74 | -34.58 to -26.90 | Yes | **** | <0.0001 |
| mRNA/PEI vs. 6x FGmRNA/PEI | -24.39 | -31.85 to -16.92 | Yes | ** | 0.0017 |
| mRNA/PEI vs. 6x FGmRNA/PEI | -24.39 | -31.85 to -16.92 | Yes | ** | 0.0017 |
| 6x FGmRNA/PEI vs. 6x FGmRNA/PEI | 0.000 | | | | |
| | | | | | |
| mRNA/PEI vs. 6x FGmRNA/PEI | -24.39 | -31.85 to -16.92 | Yes | ** | 0.0017 |
| 6x FGmRNA/PEI vs. 6x FGmRNA/PEI | 0.000 | | | | |
| | | | | | |
| E-NPs Control | | | | | |
| 24h vs. 48h | 0.3850 | -0.9895 to 1.760 | No | ns | 0.4384 |
| | | | | | |
| FGmRNA | | | | | |
| 24h vs. 48h | 13.40 | 11.40 to 15.40 | Yes | *** | 0.0002 |
| | | | | | |
| FGmRNA/PEI | | | | | |
| 24h vs. 48h | 5.923 | 2.217 to 9.628 | Yes | * | 0.0147 |
| | | | | | |
| mRNA/PEI | | | | | |
| 24h vs. 48h | 12.01 | 6.383 to 17.63 | Yes | ** | 0.0065 |
| | | | | | |
| 6x FGmRNA/PEI | | | | | |
| 24h vs. 48h | 12.53 | 9.875 to 15.19 | Yes | *** | 0.0006 |
| | | | | | |
| 6x FGmRNA/PEI | | | | | |
| 24h vs. 48h | 12.53 | 9.875 to 15.19 | Yes | *** | 0.0006 |

***Figure S9: Print screen of statistical outcome of Figure 16A and S8A 'GFP-positive Cells' in Graphpad PRISM.*** *Two-way ANOVA followed by Tukey's post-hoc test with statistical significance defined as $p < 0.05$ (*), $p < 0.01$ (**), $p < 0.001$ (***), and $p < 0.0001$ (****).*

| | | | | | |
|---|---|---|---|---|---|
| Compare cell means with others in its row and its column | | | | | |
| | | | | | |
| Number of families | 8 | | | | |
| Number of comparisons per row family | 15 | | | | |
| Number of comparisons per column family | 1 | | | | |
| Alpha | 0.05 | | | | |
| | | | | | |
| **Tukey's multiple comparisons test** | **Mean Diff.** | **95.00% CI of diff.** | **Below threshold?** | **Summary** | **Adjusted P Value** |
| | | | | | |
| 24h | | | | | |
| E-NPs Control vs. FGmRNA | -11.79 | -13.37 to -10.21 | Yes | **** | <0.0001 |
| E-NPs Control vs. FGmRNA/PEI | -7.035 | -12.34 to -1.726 | Yes | * | 0.0230 |
| E-NPs Control vs. mRNA/PEI | -19.48 | -27.22 to -11.73 | Yes | ** | 0.0035 |
| E-NPs Control vs. 6x FGmRNA/PEI | -44.39 | -50.88 to -37.90 | Yes | **** | <0.0001 |
| E-NPs Control vs. 6x FGmRNA/PEI | -44.39 | -50.88 to -37.90 | Yes | **** | <0.0001 |
| FGmRNA vs. FGmRNA/PEI | 4.758 | -2.119 to 11.63 | No | ns | 0.1288 |
| FGmRNA vs. mRNA/PEI | -7.685 | -16.53 to 1.158 | No | ns | 0.0725 |
| FGmRNA vs. 6x FGmRNA/PEI | -32.60 | -40.35 to -24.84 | Yes | *** | 0.0010 |
| FGmRNA vs. 6x FGmRNA/PEI | -32.60 | -40.35 to -24.84 | Yes | *** | 0.0010 |
| FGmRNA/PEI vs. mRNA/PEI | -12.44 | -19.10 to -5.786 | Yes | ** | 0.0086 |
| FGmRNA/PEI vs. 6x FGmRNA/PEI | -37.35 | -42.21 to -32.49 | Yes | **** | <0.0001 |
| FGmRNA/PEI vs. 6x FGmRNA/PEI | -37.35 | -42.21 to -32.49 | Yes | **** | <0.0001 |
| mRNA/PEI vs. 6x FGmRNA/PEI | -24.91 | -30.40 to -19.42 | Yes | *** | 0.0008 |
| mRNA/PEI vs. 6x FGmRNA/PEI | -24.91 | -30.40 to -19.42 | Yes | *** | 0.0008 |
| 6x FGmRNA/PEI vs. 6x FGmRNA/PEI | 0.000 | | | | |
| | | | | | |
| 48h | | | | | |
| E-NPs Control vs. FGmRNA | 1.223 | -2.369 to 4.814 | No | ns | 0.5136 |
| E-NPs Control vs. FGmRNA/PEI | -1.498 | -5.512 to 2.517 | No | ns | 0.4492 |
| E-NPs Control vs. mRNA/PEI | -7.855 | -12.61 to -3.101 | Yes | * | 0.0122 |
| E-NPs Control vs. 6x FGmRNA/PEI | -32.24 | -38.00 to -26.48 | Yes | *** | 0.0003 |
| E-NPs Control vs. 6x FGmRNA/PEI | -32.24 | -38.00 to -26.48 | Yes | *** | 0.0003 |
| FGmRNA vs. FGmRNA/PEI | -2.720 | -6.807 to 1.367 | No | ns | 0.1413 |
| FGmRNA vs. mRNA/PEI | -9.078 | -14.53 to -3.628 | Yes | * | 0.0120 |
| FGmRNA vs. 6x FGmRNA/PEI | -33.46 | -36.37 to -30.56 | Yes | **** | <0.0001 |
| FGmRNA vs. 6x FGmRNA/PEI | -33.46 | -36.37 to -30.56 | Yes | **** | <0.0001 |
| FGmRNA/PEI vs. mRNA/PEI | -6.358 | -13.94 to 1.230 | No | ns | 0.0798 |
| FGmRNA/PEI vs. 6x FGmRNA/PEI | -30.74 | -34.58 to -26.90 | Yes | **** | <0.0001 |
| FGmRNA/PEI vs. 6x FGmRNA/PEI | -30.74 | -34.58 to -26.90 | Yes | **** | <0.0001 |
| mRNA/PEI vs. 6x FGmRNA/PEI | -24.39 | -31.85 to -16.92 | Yes | ** | 0.0017 |
| mRNA/PEI vs. 6x FGmRNA/PEI | -24.39 | -31.85 to -16.92 | Yes | ** | 0.0017 |
| 6x FGmRNA/PEI vs. 6x FGmRNA/PEI | 0.000 | | | | |
| E-NPs Control | | | | | |
| 24h vs. 48h | 0.3850 | -0.9895 to 1.760 | No | ns | 0.4384 |
| | | | | | |
| FGmRNA | | | | | |
| 24h vs. 48h | 13.40 | 11.40 to 15.40 | Yes | *** | 0.0002 |
| | | | | | |
| FGmRNA/PEI | | | | | |
| 24h vs. 48h | 5.923 | 2.217 to 9.628 | Yes | * | 0.0147 |
| | | | | | |
| mRNA/PEI | | | | | |
| 24h vs. 48h | 12.01 | 6.383 to 17.63 | Yes | ** | 0.0065 |
| | | | | | |
| 6x FGmRNA/PEI | | | | | |
| 24h vs. 48h | 12.53 | 9.875 to 15.19 | Yes | *** | 0.0006 |
| | | | | | |
| 6x FGmRNA/PEI | | | | | |
| 24h vs. 48h | 12.53 | 9.875 to 15.19 | Yes | *** | 0.0006 |

***Figure S10: Print screen of statistical outcome of Figure 16B and S8B 'Percent change' in Graphpad PRISM****. Two-way ANOVA followed by Tukey's post-hoc test with statistical significance defined as $p < 0.05$ (*), $p < 0.01$ (**), $p < 0.001$ (***), and $p < 0.0001$ (****).*

| | | | | | |
|---|---|---|---|---|---|
| 48h | | | | | |
| Control vs. E-NPs Control | 2.250 | -52.54 to 57.04 | No | ns | 0.8430 |
| Control vs. FGmRNA | 1.900 | -44.37 to 48.17 | No | ns | 0.8430 |
| Control vs. FGmRNA/PEI | 3.050 | -44.44 to 50.54 | No | ns | 0.6727 |
| Control vs. 6x FGmRNA/PEI | 4.450 | -72.26 to 81.16 | No | ns | 0.7152 |
| E-NPs Control vs. FGmRNA | -0.5000 | -1.817 to 0.8172 | No | ns | 0.4247 |
| E-NPs Control vs. FGmRNA/PEI | 0.1750 | -2.069 to 2.419 | No | ns | 0.9907 |
| E-NPs Control vs. 6x FGmRNA/PEI | 3.000 | -0.3126 to 6.313 | No | ns | 0.0650 |
| FGmRNA vs. FGmRNA/PEI | 0.6750 | -0.7837 to 2.134 | No | ns | 0.3025 |
| FGmRNA vs. 6x FGmRNA/PEI | 3.500 | -0.4754 to 7.475 | No | ns | 0.0700 |
| FGmRNA/PEI vs. 6x FGmRNA/PEI | 2.825 | -2.255 to 7.905 | No | ns | 0.2093 |
| Control | | | | | |
| 24h vs. 48h | 0.2000 | -1.071 to 1.471 | No | ns | 0.2952 |
| E-NPs Control | | | | | |
| 24h vs. 48h | -0.6000 | -2.228 to 1.028 | No | ns | 0.3255 |
| FGmRNA | | | | | |
| 24h vs. 48h | -3.600 | -4.880 to -2.320 | Yes | ** | 0.0029 |
| FGmRNA/PEI | | | | | |
| 24h vs. 48h | -2.325 | -3.960 to -0.6900 | Yes | * | 0.0202 |
| 6x FGmRNA/PEI | | | | | |
| 24h vs. 48h | -5.200 | -8.348 to -2.052 | Yes | * | 0.0134 |
| Control | | | | | |
| 24h vs. 48h | 0.2000 | -1.071 to 1.471 | No | ns | 0.2952 |
| E-NPs Control | | | | | |
| 24h vs. 48h | -0.6000 | -2.228 to 1.028 | No | ns | 0.3255 |
| FGmRNA | | | | | |
| 24h vs. 48h | -3.600 | -4.880 to -2.320 | Yes | ** | 0.0029 |
| FGmRNA/PEI | | | | | |
| 24h vs. 48h | -2.325 | -3.960 to -0.6900 | Yes | * | 0.0202 |
| 6x FGmRNA/PEI | | | | | |
| 24h vs. 48h | -5.200 | -8.348 to -2.052 | Yes | * | 0.0134 |

***Figure S11: Print screen of statistical outcome of Figure 16C and S8C 'Viability' in Graphpad PRISM.*** *Two-way ANOVA followed by Tukey's post-hoc test with statistical significance defined as $p < 0.05$ (*), $p < 0.01$ (**), $p < 0.001$ (***), and $p < 0.0001$ (****).*

| Tukey's multiple comparisons test | Mean Diff. | 95.00% CI of diff. | Below threshold? | Summary | Adjusted P Value | |
|---|---|---|---|---|---|---|
| E-NPs Control vs. L-mRNA | -14.29 | -32.66 to 4.080 | No | ns | 0.0959 | B-C |
| E-NPs Control vs. mRNA/PEI (1:0.798) | -11.57 | -23.38 to 0.2456 | No | ns | 0.0517 | B-D |
| E-NPs Control vs. mRNA/PEI (1:1.329) | -20.30 | -22.61 to -17.98 | Yes | * | 0.0211 | B-E |
| E-NPs Control vs. L-mRNA/PEI (1:0.798) | -7.928 | -18.63 to 2.770 | No | ns | 0.1081 | B-G |
| L-mRNA vs. mRNA/PEI (1:0.798) | -3.240 | -20.53 to 14.05 | No | ns | 0.2790 | C-D |
| L-mRNA vs. mRNA/PEI (1:1.329) | -11.97 | -19.76 to -4.177 | Yes | * | 0.0248 | C-E |
| L-mRNA vs. L-mRNA/PEI (1:0.798) | 6.363 | -3.638 to 16.36 | No | ns | 0.1553 | C-G |
| mRNA/PEI (1:0.798) vs. mRNA/PEI (1:1.329) | -8.730 | -18.23 to 0.7672 | No | ns | 0.0567 | D-E |
| mRNA/PEI (1:0.798) vs. L-mRNA/PEI (1:0.798) | 6.715 | -26.77 to 40.20 | No | ns | 0.2617 | D-G |
| mRNA/PEI (1:1.329) vs. L-mRNA/PEI (1:0.798) | 15.45 | -27.54 to 58.43 | No | ns | 0.1488 | E-G |

***Figure S13: Print screen of statistical outcome of Figure 15B and S7B 'Percent change' in Graphpad PRISM.*** *One-way ANOVA followed by Tukey's post-hoc test with statistical significance defined as $p < 0.05$ (*), $p < 0.01$ (**), $p < 0.001$ (***), and $p < 0.0001$ (****).*

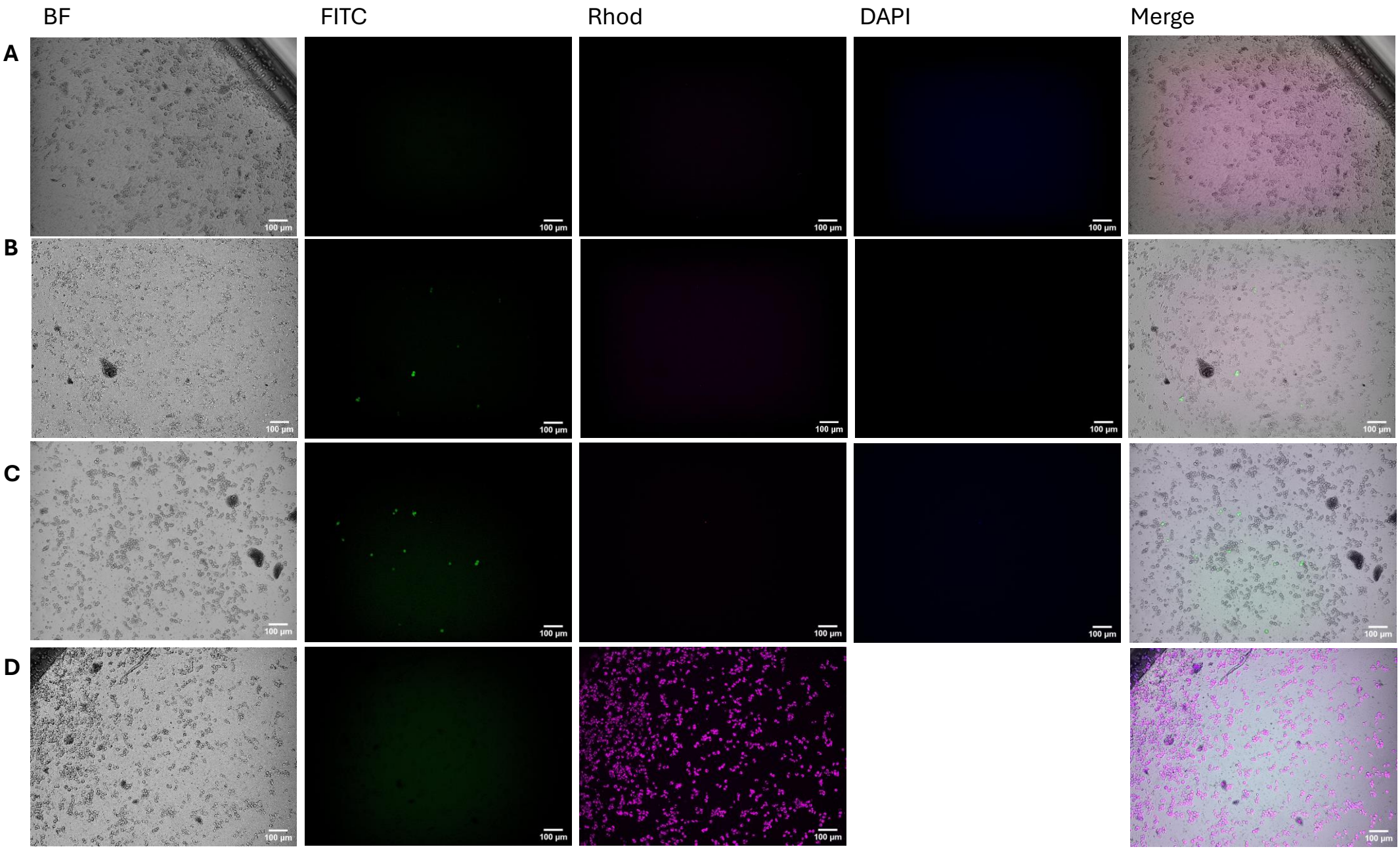


***Figure S14: Fluorescent imaging of GFP transfection of RAW macrophages with mRNA NP batches 24 h post-transfection.*** *RAW macrophages were incubated for 24h with 1,2mg of NPs per well and imaged post-treatment.* ***A:*** *E-NPs (batch WTG08) as control, no fluorescence was observed in the chosen channels.* ***B:*** *mRNA/PEI (1:1.329 w/w) NPs (batch WTG25), a couple of cells showed fluorescence in the FITC channel indicating GFP expression.* ***C:*** *1:0.798 w/w mRNA/PEI (batch WTG24), multiple green-fluorescent cells were observed at different intensities, while no Cy3 fluorescence was present.* ***D:*** *L-mRNA (batch WTG23), none of the observed cells showed GFP fluorescence, however close to all cells contained Cy3 fluorescence in the Rhod channel. Images were adjusted with FIJI ImageJ.*

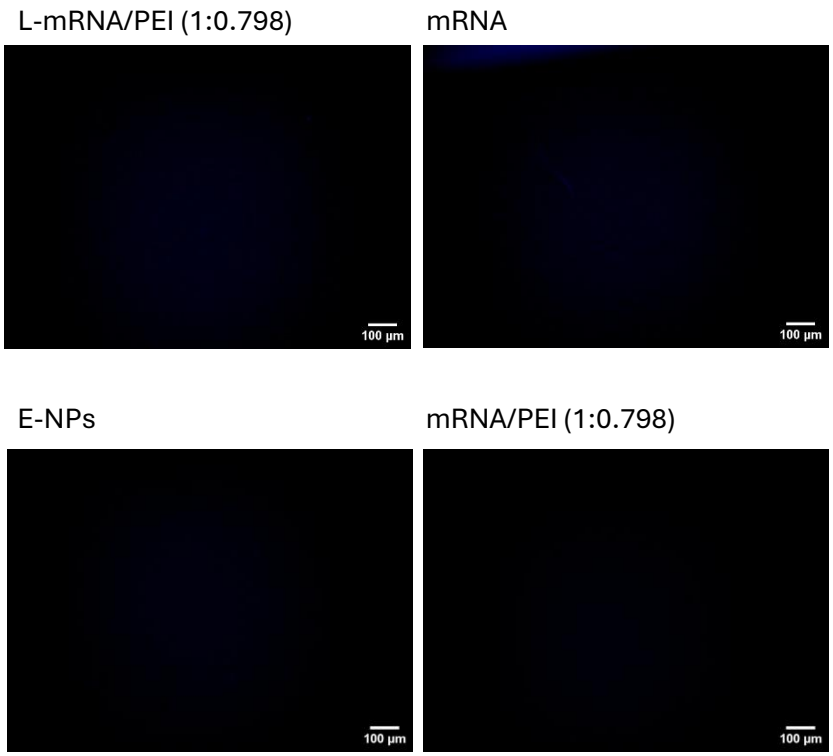


***Figure S15: DAPI filter images of 48h condition seen in Figure 14****, no autofluorescence was observed. Images were adjusted using ImageJ.*